UNIVERSITY OF CALIFORNIA
SANTA CRUZ

STATE ESTIMATION OF A LINEAR SYSTEM ON A NETWORK SUBJECT TO SPORADIC MEASUREMENTS AND TIME-DELAYS

A thesis submitted in partial satisfaction of the
requirements for the degree of

MASTER OF SCIENCE

in

COMPUTER ENGINEERING

by

Marcello Guarro

June 2019

The Thesis of Marcello Guarro
is approved:

Professor Ricardo G. Sanfelice, Chair

Professor Abhishek Halder

Professor Chen Qian

Lori Kletzer
Vice Provost and Dean of Graduate Studies

Table of Contents

List of Figures **iv**

Abstract **vi**

1 Introduction **1**
1.1 Background and Motivation 1
1.2 Related Work 6
1.3 Outline of the Proposed Observer Algorithm 7
1.4 Contributions 8
1.5 Organization and Notation 9

2 Preliminaries on Hybrid Systems **10**

3 Problem Statement and Hybrid Modeling **12**

4 Main Results **19**
4.1 Asymptotic attractivity for nominal solutions 19
4.2 Attractivity for delay solutions with synchronized clocks 24
4.3 Attractivity for delay solutions with clocks that synchronize in finite time. 28

5 Examples **32**

6 Conclusion **36**

Bibliography **37**

A Properties of $\mathcal{H}_a$ for Synchronized Clocks **41**

List of Figures

1.1 Block diagram of the networked plant-observer system. 2

1.2 The evolution of the estimation error with respect to time. The vertical dashes represent the jumps of $\hat{z}$ according to $\hat{z}^+$. 3

1.3 The evolution of the estimation error with respect to real time with the observer law that rejects delayed measurements. The vertical dashes represent the resets of $\hat{z}$ according to $\hat{z}^+$ in (1.4). 5

3.1 Diagram of the observer $\mathcal{H}_a$ and clock synchronization $\mathcal{H}_b$ subsystems and their interconnection. 13

4.1 Plot of ϕ^r and ϕ solution trajectories. 21

4.2 Plot of the Lyapunov trajectories of ϕ^r and ϕ. 28

5.1 The evolution of the estimation error with respect to hybrid time. The vertical dashes represent the resets of $\hat{z}$ according to $\hat{z}^+$ in (1.5). 33

5.2 Plot of the error on the state components (left) and of $V(x)$ evaluated along the trajectories of ϕ^{nom} and ϕ^δ (right) for synchronized clocks from Example 5.0.2. Furthermore, a plot of the bound from (4.10) plotted in black. 33

5.3 Plot of the error on the state components (left) and of $V(x)$ evaluated along the trajectories of ϕ^{nom} and ϕ^δ (right) for the case of initially mismatched clocks τ_P and τ_O. 34

5.4 Plot of he error norm for ϕ^{nom} and ϕ^δ with drifting τ_O clock. 35

A.1 Diagram of $\mathcal{H}_a$ in isolation. 41

A.2 Sample plot of the two solutions ϕ^{nom} and ϕ^{δ} showing the overlap over particular intervals of flow. 43

Abstract

State Estimation of a Linear System on a Network subject to Sporadic Measurements and Time-Delays

by

Marcello Guarro

This thesis proposes a hybrid observer for state estimation over a network. The network provides delayed measurements of the output of the plant at time instants that are not necessarily periodic and are accompanied by timestamps provided by a clock that synchronizes with the clock of the observer in finite time. The proposed observer, along with the plant and communication network, are modeled by a hybrid dynamical system that has two timers, a logic variable, and two memory states to capture the mechanisms involved in the events associated with sampling and arrival of information, as well as the logic in the estimation algorithm. The hybrid model also includes a generic clock synchronization scheme to cope with a mismatch between the clocks at the plant and the observer. Convergence properties of the estimation error of the system are shown analytically and supported by numerical examples.

Chapter 1

Introduction

1.1 Background and Motivation

In recent years, there has been continued interest in state estimation and control over networks due to the growing viability of low cost digital communication networks in settings and applications with deterministic constraints. The implementation of such networks as a communication medium for control systems has posed challenges in controller and observer design when the inherent characteristics and limitations of networks are considered. The problems posed by these challenges has given way to the interdisciplinary field of Networked Control Systems (NCSs) that deals, specifically, with the problems posed by these challenges, see [1].

Network disturbances in the form of packet delays and dropouts can often degrade control system performance and may, in some cases, destabilize the system if not properly accounted for, see [2]. Many of the constraints and disturbances introduced by networks are circumvented with the implementation of deterministic friendly networking protocols (e.g., CAN-bus, FlexRay, TTP, etc.), see [3]. However, in cases were such protocols prove impracticable, a model-based design of the system with assumptions on network disturbances may be the only approach. This thesis addresses the latter scenario.

For the model-based design setting, we consider a continuous-time linear system, given by

$$\begin{aligned} \dot{z} &= Az \\ y &= Mz \end{aligned} \tag{1.1}$$

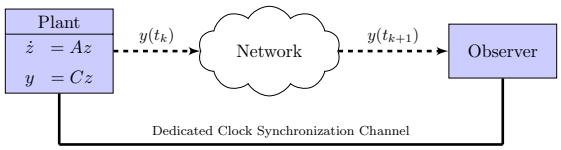

Figure 1.1: Block diagram of the networked plant-observer system.

where $z \in \mathbb{R}^n$ is the system state and $y \in \mathbb{R}^m$ is the measured output. The matrices A and M are constant and of appropriate dimensions. Now, consider a network-connected observer designed to generate estimates $\hat{z}$ of the system state z utilizing measurements y sampled and broadcast at random times t_k, $k \in \mathcal{I}_m$, where

$$\mathcal{I}_m := \{2i + 1 : i \in \mathbb{N}\}$$

and $\mathbb{N}$ denotes the set of natural numbers, i.e., $\mathbb{N} = \{0, 1, 2, ..\}$. Moreover, we assume the network experiences variable transmission delays: the sampled measurements $y(t_k)$ are available only at random times t_k, $k \in \mathcal{I}_d$, where

$$\mathcal{I}_d := \{2i : i \in \mathbb{N}\} \setminus \{0\}$$

See Fig. 1.1 for a block diagram representation of the proposed networked observer system.

The measurement sampling and arrival events are described by a strictly increasing unbounded sequence of instants $\{t_k\}_{k=0}^{\infty}$ where

$$\begin{aligned} 0 \leq t_1 &\leq T_2^N \\ T_1^N \leq t_k - t_{k-2} &\leq T_2^N \quad \forall k \in \mathcal{I}_m \\ 0 \leq t_k - t_{k-1} &\leq T^d \quad \forall k \in \mathcal{I}_d \end{aligned} \tag{1.2}$$

with $t_0 = 0$. The scalars T_1^N and T_2^N define the minimum and maximum allowable transfer interval (MATI), respectively, while T^d is an upper bound on the transmission delay and are such that $T_2^N \geq T_1^N \geq T^d > 0$.

The goal is to generate an estimate of the state $\hat{z} \in \mathbb{R}^n$, using the measured output from the plant in an impulsive-type Luenberger observer. The algorithm presented by Ferrante et. al in [4] is a viable solution for the scenario where the measurement output is aperiodic and instantaneously available. However, it is not robust to small delays when the plant state grows unbounded.

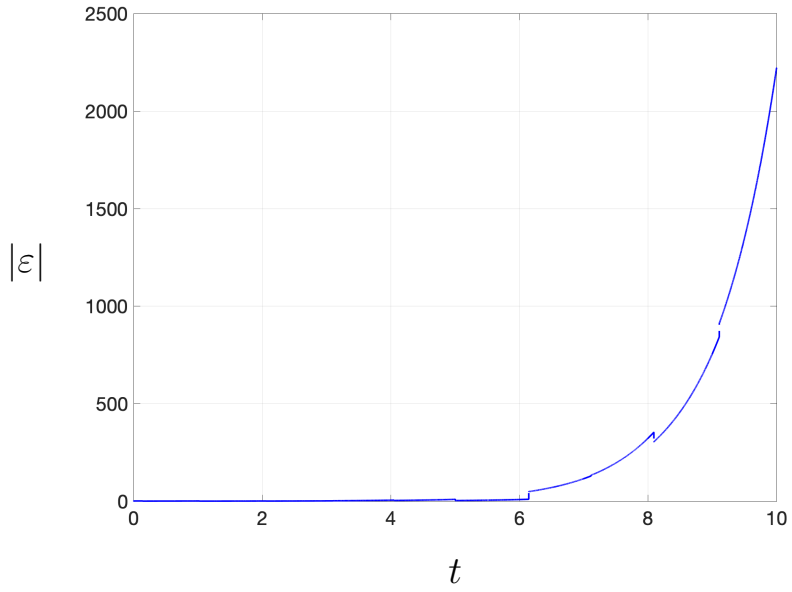

Figure 1.2: The evolution of the estimation error with respect to time. The vertical dashes represent the jumps of $\hat{z}$ according to $\hat{z}^+$.

To show this, consider the impulsive observer,

$$\begin{cases} \dot{\hat{z}}{=}A\hat{z} & \forall t \notin \{t_k\}_0^{+\infty} \\ \hat{z}(t_k^+){=}\begin{cases} \hat{z}(t_k){+}L(y(t_{k-1}){-}M\hat{z}(t_k)) & \forall t{=}t_k, k \in \mathcal{I}_d \\ \hat{z}(t_k) & \forall t{=}t_k, k \in \mathcal{I}_m \end{cases} \end{cases} \tag{1.3}$$

where $L \in \mathbb{R}^{m\times n}$ is a gain matrix designed according to the algorithm in [4] such that the estimation error $\varepsilon := z - \hat{z}$ converges to zero.

Now, consider the scalar example from [4] given by the following system data: $A = 1$, $M = 1$ with chosen constants $T_1 = T_2 = 1$ and $L = 1 - e^{-1}$ designed such that the conditions outlined in [4] are satisfied. Then, let $T^d = 0.2$. Simulating the observer in (1.3), Figure 1.2 shows that the norm of the estimate error $\varepsilon = z - \hat{z}$ for the given data diverges due to the small delay introduced on the measurements. The observer proposed in this work solves this problem.

Now suppose the measurements $y(t_k)$ are accompanied by a timestamp $\ell_t(t_k)$. Then, consider the observer from (1.3) modified such that only instantaneous mea-

surement arrivals are used and those that have incurred a delay during transmission are ignored by the observer

$$\begin{cases} \dot{\hat{z}} = A\hat{z} & \forall t \notin \{t_k\}_0^\infty \\ \hat{z}(t_k^+) = \begin{cases} \hat{z}'(t_k^+) & \forall k \in \mathcal{I}_d \\ \hat{z}(t_k) & \forall k \in \mathcal{I}_m \end{cases} \end{cases} \tag{1.4}$$

where

$$\hat{z}'(t_k^+) = \begin{cases} \hat{z}(t_k) + L(y(t_{k-1}) - M\hat{z}(t_k)) & \text{if } \ell_t(t_{k-1}) = t_k \\ \hat{z}(t_k) & \text{if } \ell_t(t_{k-1}) \neq t_k \end{cases}$$

Note that for this observer scheme, a local clock at the observer synchronized with the plant clock is necessary for the algorithm to identify the delayed measurements. Even then, this observer does not reconstruct the state for all scenarios.

In fact, consider the same system data as above, namely $A = 1$, $M = 1$, $L = 1 - e^{-1}$ with constants $T_1 = T_2 = 1$. Then, let $T^d = 0.2$. Simulating the observer in (1.4), at times $t \in \{t_k\}_{k=0}^\infty$ the estimate is corrected and the error decreases, but when the measurements are delayed then the estimate provided by the observer does not converge. Figure 1.3 shows the behavior of the norm of the estimate error $\varepsilon = z - \hat{z}$ under such a scenario. The observer proposed in this work also solves this problem.

The issues outlined in the aforementioned examples motivate a hybrid observer design, with a clock synchronization scheme, that properly uses the information received even under the scenario of measurement delays.

As demonstrated by the preceding examples, the prime challenges to solve this problem are given as follows:

1. *Aperiodic measurement broadcast events at unknown times:* the event times at which plant measurements are sampled and broadcast to the network for the observer are not known a priori. In addition, the time elapsed between each broadcast event time instant is variable within a minimum and maximum allowable transfer interval.

2. *Variable transmission delays:* the network is treated as a non-ideal communication medium hence, it is subject to latency delays that are also assumed to be variable.

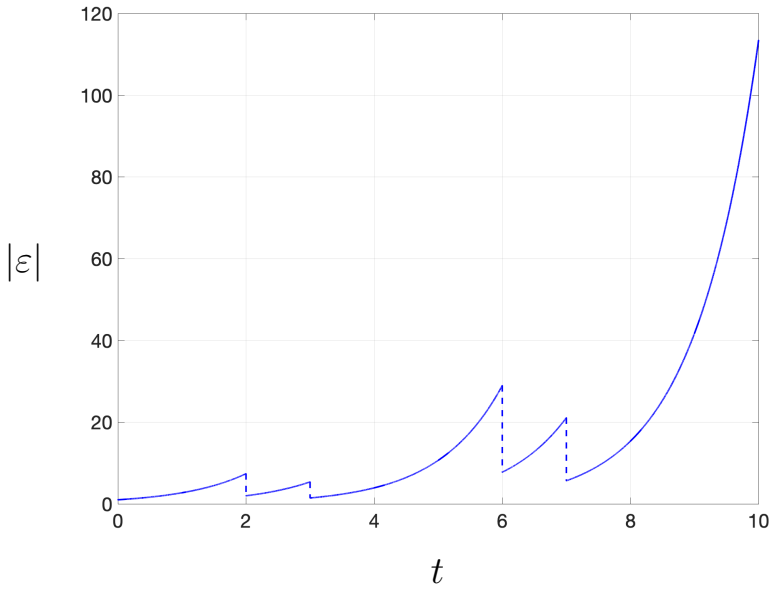

Figure 1.3: The evolution of the estimation error with respect to real time with the observer law that rejects delayed measurements. The vertical dashes represent the resets of $\hat{z}$ according to $\hat{z}^+$ in (1.4).

Similar to the aperiodicity of the broadcast event times, the time-elapsed between between measurement broadcast and arrival is not fixed nor is it known a priori.

3. *De-Synchronized network clocks:* due to the variability in the broadcast and arrival times of measurements, consensus between networked agents on the system time frame is necessary to maintain the temporal ordering of measurement sampling events. However, imperfections in the dynamics and initialization of the clocks for each agent can lead to de-synchronization and thus a lack of consensus on event ordering.

1.2 Related Work

State estimation and, in particular, feedback control in networked settings has received much attention over the years and has been posed in a variety of problem formulations and scenarios. Initial works on the subject examined traditional settings of periodic sampling and fixed delay, for which the system is treated as a time-invariant discrete-time system. Stability of the system can be easily established by checking that the eigenvalues of the state transition matrix for the closed-loop system have magnitude less than one. An example of such an approach is explored and argued in [5]. However, the approach proves limiting in cases where the delay in the system communication is variable and no longer deterministic.

The nondeterministic scenario considers the problem of networked control system that exhibit periodic sampling with variable communication delay or similarly, aperiodic sampling with fixed communication delay. Results of such scenarios have been given from a variety of control theoretic disciplines. Discrete-time approaches via system integration or tractable stability conditions using linear matrix inequalities (LMIs) have seen much popularity in the networked control setting as exhibited in the works of [2], [6], and [7]. For the state estimation and observer design setting, see [8] and [9]. The problem has also been formulated into a time-delay setting where Lyapunov-Krasovskii functionals and Razumikhin-type methods are used to show system stability. Examples of such approaches are exhibited in [10], [11], and [12].

Of particular interest, however, is the problem formulation in a hybrid systems set-

ting that considers the continous dynamics of the system between the impulsive events of measurement sampling and control actuation. General solutions using a hybrid systems approach have been presented in the works of [13] and [14] where design conditions have been given to ensure system stability. For the observer case we have the results of [15] and those of [4], [16], and [17] that give design conditions using linear matrix inequalities.

A related nondeterministic scenario that has received less attention, of which is the interest of this thesis, is that of aperiodic sampling and variable delay. The authors in [18] consider a control system setting for such a problem utilizing a discrete-time approach. They show that the system can be rendered stable using a Lyapunov function that considers both sampling and measurement delay intervals that are assumed to be bounded. However, finding numerical solutions is only feasible for particular restrictions on the interval bounds and proves to be intractable for the general case.

In the context of systems with mismatched clocks, the authors of [19] provide LMI design conditions to design a controller that renders a plant with uncertain dynamics stable in a networked control setting where clock synchronization errors exist.

1.3 Outline of the Proposed Observer Algorithm

Motivated by the challenges outlined in 1.1, we propose the following a new hybrid strategy for reconstructing the state z:

- Measurements y broadcast at times t_k, $k \in \mathcal{I}_d$, are accompanied by a time-stamp $\ell_t(t_k) = t_k$.
- When the subsequent measurements arrive at times t_k, $k \in \mathcal{I}_m$, the current state estimate $\hat{z}(t_k)$ is backward propagated to $\hat{z}(t_{k-1})$ via

  $$\hat{z}(t_{k-1}) = e^{-A\delta_k}\hat{z}(t_k)$$

  where $\delta_k := t_k - \ell_t(t_{k-1})$ is the incurred delay.
- With the estimate $\hat{z}(t_k)$ retrieved, the reset law in (1.3) is applied, namely,

  $$\begin{aligned}\hat{z}^* &= \hat{z}(t_{k-1}) + L\big(y(t_{k-1}) - M\hat{z}(t_{k-1})\big) \\ &= e^{-A\delta_k}\hat{z}(t_k) + L\big(y(t_{k-1}) - Me^{-A\delta_k}\hat{z}(t_k)\big)\end{aligned}$$

where $\hat{z}^*$ is the value of the estimate obtained after the reset law is applied.

- The reset estimate $\hat{z}^*(t_{k-1}^+)$ is then forward propagated to t_k

$$\hat{z}^*(t_k) = e^{A\delta_k}\hat{z}^*$$

Combining the above steps into a model as in (1.3), the proposed hybrid observer law can be summarized as follows:

$$\begin{cases} \dot{\hat{z}} = A\hat{z} & \forall t \notin \{t_k\}_0^\infty \\ \hat{z}(t_k^+) = \begin{cases} \hat{z}(t_k) + e^{A\delta_k}L\big(y(t_{k-1}) - Me^{-A\delta_k}\hat{z}(t_k)\big) & \forall t{=}t_k, k \in \mathcal{I}_d \\ \hat{z}(t_k) & \forall t{=}t_k, k \in \mathcal{I}_m \end{cases} \end{cases} \tag{1.5}$$

Excluding the measurement output y, the proposed strategy relies on the accessibility to information on the delay interval δ_k, which assumes both plant and observer are operating on the same time scale. Therefore, in addition to the presented strategy for generating state estimates, the observer incorporates a clock synchronization scheme, that guarantees finite time clock synchronization, to ensure accessibility to the delay interval when the measurements are time-stamped.

The continuous and discrete nature of the proposed observer in addition to the interconnection of a clock synchronization scheme, makes it an ideal candidate to model it as a hybrid system using the framework in [20].

1.4 Contributions

This thesis proposes a hybrid observer interconnected with a hybrid clock synchronization scheme that estimates the state of a linear plant over a network subject to latency delays. More specifically, building on the results in [4], this thesis introduces a hybrid system model of an NCS that possesses the ability to capture aperiodic sensor sampling with communication delays and desynchronized node clocks utilizing the framework presented in [20].

In particular, we present results that show the viability of our proposed solution by providing analysis on the asymptotic attractivity of the system trajectories to a set of interest for a few scenarios. We first show the feasibility of our solution by presenting results for the ideal case where there is no incurred delay in the transmission of the

measurements and we assume the observer clocks are synchronized. We then provide results with the incurred delay but we assume the clocks at the plant and observer are synchronized. Finally, our third contribution is an attractivity analysis of the estimation error for the case where clocks at the plant and observer are not initially synchronized but synchronize in finite time while being subjected to measurement delays.

The inability to apply existing results to an NCS that considers the challenges outlined in Section 1.1, motivates the work in this thesis and constitutes a noted discrepancy in the existing literature. Moreover, we are not aware of any such result that considers concurrency of the measured output via the inclusion of a clock synchronization scheme.

1.5 Organization and Notation

The remainder of this thesis is organized as follows: Section 2 presents some preliminaries on hybrid systems. Section 3 presents the problem we solve and the associated hybrid model of the system. Section 4 details the main results and Section 5 outlines several numerical examples.

Notation: In this thesis the following notation and definitions will be used. $\mathbb{N}$ denotes the set of natural numbers, i.e., $\mathbb{N} = \{0, 1, 2, ..\}$. $\mathbb{N}_{>0}$ denotes the set of natural numbers not including 0, i.e., $\mathbb{N}_{>0} = \{1, 2, ..\}$. $\mathbb{R}$ denotes the set of real numbers. $\mathbb{R}_{\geq 0}$ denotes the set of non-negative real numbers, i.e., $\mathbb{R}_{\geq 0} = [0, \infty)$. $\mathbb{R}^n$ denotes n-dimensional Euclidean space. Given topological spaces A and B, $F : A \rightrightarrows B$ denotes a set-valued map from A to B. For a matrix $A \in \mathbb{R}^{n\times m}$, A^T denotes the transpose of A. For a matrix $A \in \mathbb{R}^{n\times m}$, A^* denotes the conjugate transpose of A. Given a vector $x \in \mathbb{R}^n$, $|x|$ denotes the Euclidean norm. Given two vectors $x \in \mathbb{R}^n$ and $y \in \mathbb{R}^m$, $(x, y) = [x^\mathsf{T}\ y^\mathsf{T}\ ]^\mathsf{T}$. Given a matrix $A \in \mathbb{R}^n$, $\lambda_{\max}(A)$ denotes the largest eigenvalue of A and $\lambda_{\min}(A)$ denotes the smallest eigenvalue of A. Given a matrix $A \in \mathbb{R}^n$, $|A| := \max\{\sqrt{|\lambda|} : \lambda \in \text{eig}(A^\mathsf{T}A)\}$. For two symmetric matrices $A \in \mathbb{R}^n$ and $B \in \mathbb{R}^n$, $A \succ B$ means that $A - B$ is positive definite, conversely $A \prec B$ means that $A - B$ is negative definite. Given a closed set $A \subset \mathbb{R}^n$ and closed set $B \subset A$, the projection of A onto B is denoted by $\Pi_B(A)$. Given a function $f : \mathbb{R}^n \to \mathbb{R}^m$, the range of f is given by $\text{rge } f := \{y \mid \exists\, x \text{ with } y \in f(x)\}$.

Chapter 2

Preliminaries on Hybrid Systems

We recall that a hybrid system $\mathcal{H}$ on $\mathbb{R}^n$ is composed by the following *data*:

- a set $C \subset \mathbb{R}^n$, called the flow set;
- a set-valued mapping $F : \mathbb{R}^n \rightrightarrows \mathbb{R}^n$ with $C \subset \text{dom } F$, called the flow map;
- a set $D \subset \mathbb{R}^n$, called the jump set;
- a set-valued mapping $G : \mathbb{R}^n \rightrightarrows \mathbb{R}^n$ with $D \subset \text{dom } G$, called the jump map.

Then a hybrid system $\mathcal{H} := (C, F, D, G)$ with state vector $x \in \mathbb{R}^n$ written in its compact form is given by

$$\mathcal{H} \begin{cases} \dot{x} \in F(x) & x \in C \\ x^+ \in G(x) & x \in D \end{cases} \tag{2.1}$$

Solutions to a hybrid system $\mathcal{H}$, denoted ϕ, are parameterized by (t, j) where $t \in \mathbb{R}_{\geq 0}$ defines ordinary time and $j \in \mathbb{N}$ counts the number of jumps. The evolution of a solution is described by a *hybrid arc* on a *hybrid time domain* [20]. A hybrid time domain is given by dom $\phi \subset \mathbb{R}_{\geq 0} \times \mathbb{N}$ if, for each $(T, J) \in$ dom ϕ, dom $\phi \cap ([0, T] \times \{0, 1, ..., J\})$ is of the form $\bigcup_{j=0}^{J}([t_j, t_{j+1}] \times \{j\})$, with $0 = t_0 \leq t_1 \leq t_2 \leq t_{J+1}$. Moreover, we use $\mathcal{S}_{\mathcal{H}}$ to represent the set of all solutions to $\mathcal{H}$.

A solution ϕ is said to be *maximal* if its evolution cannot be extended by a period of flow or a jump and *complete* if its domain is unbounded. A hybrid system is *well-posed* if it satisfies the hybrid basic conditions in [20, Assumption 6.5]. Let $\mathcal{A} \subset \mathbb{R}^n$ be a closed set and $|x|_{\mathcal{A}} := \inf_{y \in \mathcal{A}} |x - y|$.

Definition 2.0.1. *A closed set $\mathcal{A} \subset \mathbb{R}^n$ is said to be*

- *stable for $\mathcal{H}$ if for every $\epsilon > 0$ there exists $\delta > 0$ such that every solution ϕ to $\mathcal{H}$ with $|\phi(0,0)|_{\mathcal{A}} \leq \delta$ satisfies $|\phi(t,j)|_{\mathcal{A}} \leq \epsilon$ for all $(t,j) \in \text{dom } \phi$;*
- *attractive for $\mathcal{H}$ if there exists $\mu > 0$ such that every solution ϕ to $\mathcal{H}$ with $|\phi(0,0)|_{\mathcal{A}} \leq \mu$ is complete and satisfies $\lim_{t+j\to\infty} |\phi(t,j)|_{\mathcal{A}} = 0$;*
- *asymptotically stable for $\mathcal{H}$ if both stable and attractive for $\mathcal{H}$;*
- *globally exponentially stable for $\mathcal{H}$ if there exists positive scalars $k, \lambda > 0$ such that every solution ϕ to $\mathcal{H}$ is such that $|\phi(t,j)|_{\mathcal{A}} \leq ke^{-\lambda(t+j)}|\phi(0,0)|_{\mathcal{A}}$ for all $(t,j) \in dom\ \phi$.*

When inputs are added one has similar notions as long as every static solution for every input satisfies the properties in Definition 2.0.1. For more details on hybrid systems, see [20].

Chapter 3

Problem Statement and Hybrid Modeling

The problem addressed in this thesis is as follows:

Problem 3.0.1. *Given the linear time invariant system (1.1) and positive constants* $0 < T^d \leq T_1^N \leq T_2^N$*, design a hybrid algorithm including the hybrid observer in (1.5) such that the resulting closed-loop system* $\mathcal{H}$ *is such that* $\hat{z}(t,j) - z(t,j)$ *converges to zero as* $t + j \to \infty$*.*

To solve this problem, we employ the hybrid observer in (1.5). The design of this hybrid algorithm requires finding a proper choice of the matrix L. To find such an L, we consider the LMI condition presented in [4] for which an algorithm is given to solve. The hybrid algorithm proposed in this thesis also includes provisions for a clock synchronization algorithm the clocks determining time for both the plant and the observer.

Next, we define the hybrid model that provides the framework and solution to Problem 3.0.1. The model is constructed such that the observer defined in (1.5) is recast with the dynamics of the network as a hybrid system with a set-valued jump map. Moreover, provisions are included to facilitate the inclusion of a clock synchronization strategy to ensure proper function of the hybrid observer. To build such a model, we treated the observer and clock synchronization strategy as individual but interconnected subsystems. Figure 3.1 describes such a system where, $\mathcal{H}_a$ is the plant-observer subsystem and $\mathcal{H}_b$ is the clock synchronization subsystem. With the chosen design of $\mathcal{H}$, the system can be viewed as the interconnection of two hybrid subsystems.

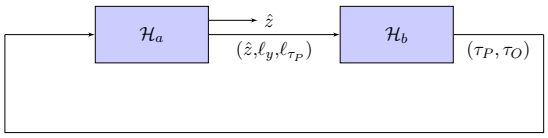

Figure 3.1: Diagram of the observer $\mathcal{H}_a$ and clock synchronization $\mathcal{H}_b$ subsystems and their interconnection.

To model the aperiodic measurement sampling of the plant, a timer variable τ_N is used. Between measurement sampling events the timer flows with dynamics given by $\dot{\tau}_N = -1$ and when $\tau_N = 0$, the state τ_N is reset to a value in the interval $[T_1^N, T_2^N]$. The transmission delay is modeled by an additional timer τ_δ with dynamics $\dot{\tau}_\delta = -q$. Here $q \in \{0, 1\}$ is a discrete variable used to control the dynamics of τ_δ such that the timer is active only following measurement broadcast events. More precisely, $q = 1$ denotes an active measurement in the network and $q = 0$ denotes the absence of such a measurement in the network. Thus, when $\tau_N = 0$, τ_δ is reset to a point in the interval $[0, T^d]$ and q is reset to 1. When $\tau_\delta = 0$, indicating measurement arrival, τ_δ is reset to -1 and q is reset to 0. Having the timers τ_N and τ_δ defined in this way, with the addition of q, enforces the constraints defined in (1.2) for broadcast and arrival events.

Additionally, we let ℓ_y and ℓ_{τ_P} represent memory states that define the plant measurement data and associated timestamp, respectively. The states τ_P and τ_O represent the global clocks for the respective plant and observer. The state μ represents the state variables for a clock synchronization algorithm.

Then, we define the state vector of the interconnection of the plant and the observer system $\mathcal{H}$ as $x := (x_a, x_b) \in \mathcal{X}_a \times \mathcal{X}_b =: \mathcal{X}$ where $x_a := (z, \hat{z}, \tau_N, \tau_\delta, q, \ell_y, \ell_{\tau_P}) \in \mathcal{X}_a$, $x_b := (\tau_P, \tau_O, \mu) \in \mathcal{X}_b$ with $\mathcal{X}_a := \mathbb{R}^n \times \mathbb{R}^n \times [0, T_2^N] \times \big(\{-1\} \cup [0, T^d]\big) \times \{0, 1\} \times \mathbb{R}^m \times \mathbb{R}_{\geq 0}$ and $\mathcal{X}_b := \mathbb{R}_{\geq 0} \times \mathbb{R}_{\geq 0} \times \mathcal{M}$. The closed set $\mathcal{M}$ defines possible values of μ. The flow map is given by

$$F(x) := \begin{bmatrix} F_a(x_a) \\ F_b(x_b, \hat{z}, \ell_y, \ell_{\tau_P}) \end{bmatrix} \quad \forall x \in C$$

where

$$F_a(x_a) := \big(Az, A\hat{z}, -1, -q, 0, 0, 0\big)$$

and

$$F_b(x_b, \hat{z}, \ell_y, \ell_{\tau_P}) := \big(1, 1, F_s(x_b, \hat{z}, \ell_y, \ell_{\tau_P})\big)$$

with F_s governing the continuous dynamics of μ. The flow set C is defined as $C := C_a \cap C_b$ where $C_a := C_{a_1} \cup C_{a_2}$ and

$$C_{a_1} := \{x \in \mathcal{X} : q = 0, \tau_\delta = -1\}$$
$$C_{a_2} := \{x \in \mathcal{X} : q = 1, \tau_\delta \in [0, T^d]\}$$

and C_b is the flow set defined by the clock synchronization algorithm. The jump map is given by

$$G(x) := \begin{bmatrix} G_a(x_a, \tau_P, \tau_O) \\ G_b(\hat{z}, \ell_y, \ell_{\tau_P}, x_b) \end{bmatrix} \quad \forall x \in D$$

where G_a is defined as

$$G_a(x_a, \tau_P, \tau_O) := \begin{cases} G_1(x_a, \tau_P) & \text{if } x \in D_{a_1} \setminus D_b \\ G_2(x_a, \tau_O) & \text{if } x \in D_{a_2} \setminus D_b \\ x_a & \text{if } x \in D_b \backslash (D_{a_1} \cup D_{a_2}) \\ \{x_a, G_1(x_a, \tau_P)\} & \text{if } x \in D_{a_1} \cap D_b \\ \{x_a, G_2(x_a, \tau_O)\} & \text{if } x \in D_{a_2} \cap D_b \end{cases}$$

for each $x \in D$

$$G_1(x_a, \tau_P) = \begin{bmatrix} z \\ \hat{z} \\ [T_1^N, T_2^N] \\ [0, T^d] \\ 1 \\ Mz \\ \tau_P \end{bmatrix} \forall (x_a, \tau_P) : x \in D_{a_1}$$

$$G_2(x_a, \tau_O) = \begin{bmatrix} z \\ \hat{z} + e^{A(\tau_O - \ell_{\tau_P})} L\big(\ell_y - M e^{-A(\tau_O - \ell_{\tau_P})} \hat{z}\big) \\ \tau_N \\ -1 \\ 0 \\ \ell_y \\ \ell_{\tau_P} \end{bmatrix}$$

for each (x_a, τ_O) such that $x \in D_{a_2}$, where

$$D_{a_1} := \{x \in \mathcal{X} : \tau_N = 0, q = 0\}$$
$$D_{a_2} := \{x \in \mathcal{X} : \tau_\delta = 0, q = 1\}$$

In the definitions above, G_b and D_b, respectively, define the jump map and jump set for the clock synchronization algorithm. The resulting jump set is

$$D := D_a \cup D_b$$

where

$$D_a := D_{a_1} \cup D_{a_2}$$

The hybrid system data above now define $\mathcal{H}$ as follows

$$\mathcal{H} = (C, F, D, G) \tag{3.1}$$

Separating the clock synchronization from the system, one has a subsystem that is comprised only of the plant, observer, and network dynamics, denoted by

$$\mathcal{H}_a = (C_a, F_a, D_a, G_a) \tag{3.2}$$

Conversely, the hybrid subsystem denoted by

$$\mathcal{H}_b = (C_b, F_b, D_b, G_b) \tag{3.3}$$

models the clock dynamics and synchronization algorithm.

For several of the results that follow, we consider the hybrid system $\mathcal{H}_a$ with $D_b = \emptyset$. Observe that $\mathcal{H}_a$ with $D_b = \emptyset$ has data

$$\begin{aligned}&\Big(C_a, F_a, D_a\big|_{D_b=\emptyset}, G_a\big|_{D_b=\emptyset}\Big)\\ &\qquad = \left(C_a, F_a, D_{a_1} \cup D_{a_2}, \begin{cases} G_1(x_a, \tau_P) & \text{if } x \in D_{a_1} \\ G_2(x_a, \tau_O) & \text{if } x \in D_{a_2} \end{cases}\right)\end{aligned}$$

Definition 3.0.1. *A solution $\phi \in \mathcal{S}_{\mathcal{H}_a}$ is a nominal maximal solution if it belongs to the subset of maximal solutions defined by*

$$\mathcal{S}^{\text{nom}}_{\mathcal{H}_a} := \left\{\phi \in \mathcal{S}_{\mathcal{H}_a} : \text{rge } \phi_{\tau_\delta} \subset \{0, -1\}\right\} \tag{3.4}$$

where ϕ_{τ_δ} is the τ_δ component of ϕ. Additionally, we say that a solution $\phi \in \mathcal{S}_{\mathcal{H}_a}$ is a delay maximal solution if it belongs to the subset of maximal solutions defined by $\mathcal{S}^{\delta}_{\mathcal{H}_a} := \mathcal{S}_{\mathcal{H}_a} \setminus \mathcal{S}^{\text{nom}}_{\mathcal{H}_a}$.

Qualitatively, one can interpret solutions belonging to $\mathcal{S}^{\text{nom}}_{\mathcal{H}_a}$ as a representation of the scenario where the measurements are free of transmission delays. For a given $\phi \in \mathcal{S}_{\mathcal{H}_a}$, when the timer τ_N expires (i.e., $\tau_N = 0$) the state jumps according to G_1. As a consequence of (3.4), the τ_δ component of the respective ϕ_{τ_δ} solution is mapped to zero following the construction of G_1. Then, nominal maximal solutions jump from D_{a_1} to D_{a_2}, resulting in a subsequent jump with no flow between the two jumps.

Remark 3.0.2. *Definition 3.0.1 applies to both $\mathcal{H}_a$ and $\mathcal{H}$. Thus, we let $\mathcal{S}^{\text{nom}}_{\mathcal{H}}$ denote the set of nominal maximal solutions to $\mathcal{H}$ and $\mathcal{S}^{\delta}_{\mathcal{H}} = \mathcal{S}_{\mathcal{H}} \setminus \mathcal{S}^{\text{nom}}_{\mathcal{H}}$ denote the set of delay solutions to $\mathcal{H}$.*

With the hybrid system defined, the next two results establish existence of solutions to $\mathcal{H}_a$ and that every maximal solution to $\mathcal{H}_a$ is complete.

Lemma 3.0.3. *The hybrid system $\mathcal{H}_a$ with $D_b = \emptyset$ satisfies the hybrid basic conditions in [20, Assumption 6.5].*

Proof. The following hold:

- (A1) in [20, Assumption 6.5] holds since C_a and D_a are closed sets.
- (A2) in [20, Assumption 6.5] holds since F_a is outer semicontinuous and bounded relative to C_a.
- (A3) in [20, Assumption 6.5] holds since $G_a\big|_{D_b=\emptyset}$ is an outer semicontinuous construction using continuous functions G_1 and G_2. In fact, the set of points where the mappings G_1 and G_2 are applied are mutually exclusive due to $D_{a_1} \cap D_{a_2} = \emptyset$. Then, $G_a\big|_{D_b=\emptyset} : \mathcal{X}_a \rightrightarrows \mathcal{X}_a$ is outer semicontinuous and locally bounded relative to D_a and $D_a \subset \text{dom } G_a$.

Thus, $\mathcal{H}_a$ with $D_b = \emptyset$ satisfies the hybrid basic conditions. □

Lemma 3.0.4. *The data (C_a, F_a, D_a, G_a) of $\mathcal{H}_a$ with $D_b = \emptyset$ and inputs (τ_P, τ_O) is such that*

1. *$G_a(x_a, \tau_P, \tau_O) \subset C_a \cup D_a$ for all $(x_a, \tau_P, \tau_O) : x \in D_a$*
2. *$F_a(x_a) \subset T_{C_a}(x_a)$ for all $(x_a, \tau_P, \tau_O) : x \in C_a \setminus D_a$*

Proof. To prove item 1), pick $x \in D_a$

- If $x \in D_{a_1}$, since $D_b = \emptyset$ $G_a(x_a, \tau_P, \tau_O) = G_1(x_a, \tau_P) \subset D_{a_2} \subset C_{a_2}$
- If $x \in D_{a_2}$, since $D_b = \emptyset$ $G_a(x_a, \tau_P, \tau_O) = G_2(x_a, \tau_O) \subset D_{a_1} \subset C_{a_1}$

Therefore, item 1) holds.

To prove item 2), pick $x \in C_a \setminus D_a$. The tangent cone $T_{C_a}(x_a)$ is given by

$$T_{C_a}(x_a) = \begin{cases} \mathbb{R}^n \times \mathbb{R}^n \times \mathbb{R}_{\geq 0} \times \mathbb{R}_{\geq 0} \times \{0\} \times \mathbb{R}^m \times \mathbb{R}_{\geq 0} & \text{if } x_a \in \mathcal{X}_a^1 \\ \mathbb{R}^n \times \mathbb{R}^n \times \mathbb{R} \times \mathbb{R}_{\geq 0} \times \{0\} \times \mathbb{R}^m \times \mathbb{R}_{\geq 0} & \text{if } x_a \in \mathcal{X}_a^2 \\ \mathbb{R}^n \times \mathbb{R}^n \times \mathbb{R}_{\geq 0} \times \mathbb{R}_{\geq 0} \times \{0\} \times \mathbb{R}^m \times \mathbb{R}_{\geq 0} & \text{if } x_a \in \mathcal{X}_a^3 \\ \mathbb{R}^n \times \mathbb{R}^n \times \mathbb{R}_{\geq 0} \times \mathbb{R}_{\geq 0} \times \{1\} \times \mathbb{R}^m \times \mathbb{R}_{\geq 0} & \text{if } x_a \in \mathcal{X}_a^4 \\ \mathbb{R}^n \times \mathbb{R}^n \times \mathbb{R}_{\geq 0} \times \mathbb{R}_{\geq 0} \times \{1\} \times \mathbb{R}^m \times \mathbb{R}_{\geq 0} & \text{if } x_a \in \mathcal{X}_a^5 \\ \mathbb{R}^n \times \mathbb{R}^n \times \mathbb{R}_{\geq 0} \times \mathbb{R} \times \{1\} \times \mathbb{R}^m \times \mathbb{R}_{\geq 0} & \text{if } x_a \in \mathcal{X}_a^6 \end{cases}$$

where

$$\mathcal{X}_a^1 := \{x_a \in \mathcal{X}_a : q = 0, \tau_N = 0, \tau_\delta = -1\}$$
$$\mathcal{X}_a^2 := \{x_a \in \mathcal{X}_a : q = 0, \tau_N = (0, T_2^N), \tau_\delta = -1\}$$
$$\mathcal{X}_a^3 := \{x_a \in \mathcal{X}_a : q = 0, \tau_N = T_2^N, \tau_\delta = -1\}$$
$$\mathcal{X}_a^4 := \{x_a \in \mathcal{X}_a : q = 1, \tau_\delta = 0\}$$
$$\mathcal{X}_a^5 := \{x_a \in \mathcal{X}_a : q = 1, \tau_\delta = T^d\}$$
$$\mathcal{X}_a^6 := \{x_a \in \mathcal{X}_a : q = 1, \tau_\delta = (0, T^d)\}$$

By inspection $F_a(x_a) \subset T_{C_a}(x_a)$. Therefore item 2) holds. □

Lemma 3.0.5. *For every initial condition $\xi \in C_a \cup D_a$ there exists, at least, a nontrivial solution ϕ to the hybrid system $\mathcal{H}_a$ with $D_b = \emptyset$ and inputs (τ_P, τ_O) such that $\{t : (t, j) \in dom\ (\tau_P, \tau_O)\}$ is unbounded, and in particular, every maximal solution to $\mathcal{H}_a$ with $D_b = \emptyset$ and such an input is complete.*

Proof. To prove completeness of solutions we consider the extension of [20, Proposition 6.10] for the case of Hybrid Systems with inputs as presented in [21]. Given that $\mathcal{H}_a$ satisfies the hybrid basic conditions, consider an arbitrary $x_a \in C_a \cup D_a$ and recall the tangent cone $T_{C_a}(x_a)$ from the result of Lemma 3.0.5. Since F_a is independent of the inputs, by inspection, $F_a(x_a) \cap T_{C_a}(x_a) \neq \emptyset$ holds for every (x_a, τ_P, τ_O) such that $x \in C_a \setminus D_a$. Then, case (c) in [20, Proposition 6.10] can be ruled out since by item 1) Lemma 3.0.4 with $D_b = \emptyset$, $G_a(D_a) \subset C_a \cup D_a$. Case (b) in [20, Proposition 6.10] can be excluded since by inspection F_a is Lipschitz continuous on C_a. Thus, each ϕ to $\mathcal{H}_a$ with $D_b = \emptyset$ and inputs (τ_P, τ_O) such that $\{t : (t, j) \in \text{dom } \phi\}$ is unbounded must satisfy case (a) in [20, Proposition 6.10]. Observe that the notions in [20, Proposition 6.10] □

Remark 3.0.6. *For the closed-loop hybrid system $\mathcal{H}$, the completeness of maximal solutions to the interconnection between $\mathcal{H}_a$ and $\mathcal{H}_b$ depend on the hybrid system data that defines $\mathcal{H}_b$. See [20, Proposition 2.10] and [20, Proposition 6.10] for details.*

Chapter 4

Main Results

In this section, results guaranteeing convergence of the estimation error $\varepsilon := z - \hat{z}$ to zero with the proposed algorithm are given. First, attractivity is shown for nominal solutions through a comparison to the exponentially converging trajectories guaranteed by the observer in [4]. Next, a Lyapunov-like approach is used to show convergence of delay maximal solutions to a set of interest by comparing the observer trajectories of a delay maximal solution against those of a corresponding nominal maximal solution. Finally, we present a result on the convergence of the estimation error to zero for the case where the plant and observer clocks are mismatched but synchronize in finite time due to the inclusion of a clock synchronization algorithm such as the one in Example 5.0.2.

4.1 Asymptotic attractivity for nominal solutions

In this section we show that the nominal maximal solutions to $\mathcal{H}_a$ are such that the estimation error converges to zero. We prove this claim by showing that for a given set of parameters and initial conditions, the trajectories of the component $\hat{z}$ for $\mathcal{H}_a$ with synchronized clocks inputs are equivalent to those for the hybrid model presented in [4]. To this end, let us consider the hybrid system in [4] written in plant-observer

coordinates, $x_r := (z, \hat{z}, \tau_N) \in \mathbb{R}^{2n} \times \mathbb{R}_{\geq 0}$

$$F_r(x_r) := \begin{bmatrix} Az \\ A\hat{z} \\ -1 \end{bmatrix} \qquad \forall x_r \in C_r$$

$$G_r(x_r) := \begin{bmatrix} z \\ \hat{z} + LM(z - \hat{z}) \\ [T_1^N, T_2^N] \end{bmatrix} \qquad \forall x_r \in D_r$$

$$C_r := \{(z, \hat{z}, \tau) \in \mathbb{R}^n \times \mathbb{R}^n \times \mathbb{R}_{\geq 0} : \tau_N \in [0, T_2^N]\}$$
$$D_r := \{(z, \hat{z}, \tau) \in \mathbb{R}^n \times \mathbb{R}^n \times \mathbb{R}_{\geq 0} : \tau_N = 0\}$$

We denote this system as $\mathcal{H}_r$, which has the compact form

$$\mathcal{H}_r \begin{cases} \dot{x}_r = F_r(x_r) & x_r \in C_r \\ x_r^+ \in G_r(x_r) & x_r \in D_r \end{cases} \tag{4.1}$$

The hybrid time domain for solutions ϕ^r to $\mathcal{H}_r$ is given by

$$\text{dom } \phi^r = \bigcup_{j \in \mathbb{N}} \Big([t_j, t_{j+1}] \times \{j\} \Big) \tag{4.2}$$

where

$$T_1^N \leq t_{j+1} - t_j \leq T_2^N \quad \forall j \in \{k \geq 1 : k \in \mathbb{N}\}$$
$$0 \leq t_1 \leq T_2^N$$

Following [4], if matrices L and $P = P^{\mathsf{T}} \succ 0$ are such that

$$(\mathbf{I} - LM)^{\mathsf{T}} e^{A^{\mathsf{T}} v} P e^{Av} (\mathbf{I} - LM) - P \prec 0 \quad \forall v \in [T_1^N, T_2^N] \tag{4.3}$$

holds for given $T_2^N \geq T_1^N \geq 0$, then the system $\mathcal{H}_r$ has the set

$$\mathcal{A}_r := \big\{ (z, \hat{z}, \tau_N) \in \mathbb{R}^n \times \mathbb{R}^n \times [0, T_2^N] : z = \hat{z} \big\} \tag{4.4}$$

globally exponentially stable. Prior to comparing the trajectories of $\mathcal{H}_r$ and $\mathcal{H}_a$, note that $\mathcal{H}_r$ resembles system $\mathcal{H}_a$ with synchronized clock inputs τ_P and τ_O for the case where $T^d = 0$. However, as noted in Remark A.0.2, the hybrid time domain of a solution

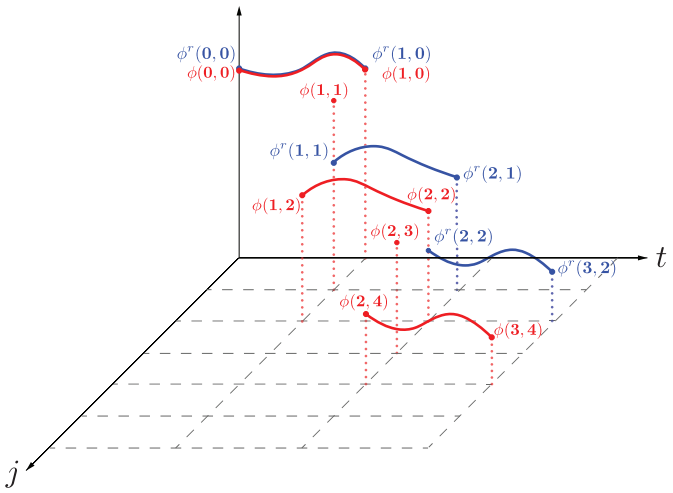

Figure 4.1: Plot of ϕ^r and ϕ solution trajectories.

ϕ^{nom} to $\mathcal{H}_a$ observes an additional jump in between periods of flow as demonstrated in Figure 4.1.

Observe that x_r is a strict subvector of x_a. Thus, for a given initial condition $\phi^r(0,0)$ for $\mathcal{H}_r$, we can consider the following initial condition for $\mathcal{H}_a$:

$$\phi(0,0) = \big(\phi_r(0,0), \phi_{\tau_\delta}(0,0), \phi_q(0,0), \phi_{\ell_y}(0,0), \phi_{\ell_{\tau_P}}(0,0)\big)$$

Moreover, for given matrices A, M, and L of appropriate dimensions, constants $0 < T_1^N \leq T_2^N$, one can pick solutions ϕ^r and ϕ belonging to $\mathcal{H}_r$ and $\mathcal{H}_a$, respectively, such that the solutions observe the same $\tau_N = 0$ triggered jump times, i.e., $\phi_{\tau_N}(t, s_\phi(j)) = \phi^r_{\tau_N}(t,j)$ for all $(t,j) \in \operatorname{dom} \phi^r$.

Using the observed relationships between the two systems, in the result that follows, we claim attractivity for nominal solutions by showing that $\phi_z \equiv \phi^r_z$ and $\phi_{\hat{z}} \equiv \phi^r_{\hat{z}}$. The proof of the result is segmented into two cases; the first addresses attractivity for solutions to $\mathcal{H}_a$ with initial condition $\phi(0,0) \in C_{a_1} \cup D_{a_1}$ or $\phi(0,0) \in \{x \in C_{a_2} \cup D_{a_2} : \ell_y = Mz, \ell_{\tau_P} = \tau_P\}$, the second address attractivity for solutions with initial condition $\phi(0,0) \in \{x \in C_{a_2} \cup D_{a_2} : \ell_y \neq Mz, \ell_{\tau_P} \neq \tau_P\}$. A separate proof for the second case is necessary to address the scenario of incorrectly initialized memory states that could lead to an "incorrect" observer law update when a jump according to G_2 is triggered. To this end, we define sets $\mathcal{W}_1 := C_{a_1} \cup D_{a_1}$ and $\mathcal{W}_2 := \{x \in C_{a_2} \cup D_{a_2} : \ell_y = Mz, \ell_{\tau_P} =$

$\tau_P(0,0)\}$. Then solutions ϕ to $\mathcal{H}_a$ with $\phi(0,0) \in \mathcal{W}_1 \cup \mathcal{W}_2$ we refer to as *conventional* solutions and for solutions with $\phi(0,0) \in (C_a \cup D_a) \setminus (\mathcal{W}_1 \cup \mathcal{W}_2)$ we refer to as *non-conventional*.

Proposition 4.1.1. *Given hybrid systems $\mathcal{H}_r$ in (4.1) and $\mathcal{H}_a$ in (3.2) with $D_b = \emptyset$ and input pair $\tau_P \equiv \tau_O$ such that $\{t : (t,j) \in dom\ (\tau_P, \tau_O)\}$ is unbounded, suppose that there exist $P = P^\top \succ 0$ such that T_2^N, T_1^N, L, and M satisfy condition (4.3). Then, for $T^d = 0$, each solution ϕ to $\mathcal{H}_a$ with $D_b = \emptyset$ and input pair $\tau_P \equiv \tau_O$ is such that*

$$\lim_{t+j\to\infty} |\phi(t,j)|_{\mathcal{A}_a} = 0$$

where

$$\mathcal{A}_a := \mathcal{A}_r \times \big(\{-1\} \cup [0, T^d]\big) \times \{0,1\} \times \mathbb{R}^m \times \mathbb{R}_{\geq 0} \tag{4.5}$$

Proof. Pick solutions ϕ^r and ϕ with initial conditions $\phi^r(0,0) \in C_r \cup D_r$ and $\phi(0,0) \in \{(\phi^r(0,0), \tau_\delta, q, \ell_y, \ell_{\tau_P}) \in C_a \cup D_a : \ell_y = Mz\}$ such that

$$\phi_{\tau_N}(t,j) = \phi^r_{\tau_N}(t, r_\phi(j)) \qquad\qquad \forall (t,j) \in \text{dom } \phi$$

where $r_{\phi^r}(j) := 2j$ is a parameterization function that maps a solution ϕ^r to $\mathcal{H}_r$ onto the hybrid time domain of ϕ to $\mathcal{H}_a$.

• Proof of Conventional Case

Following ϕ^r from $\phi^r(0,0)$, if $\phi^r(t,j) \in C_r$ it flows according to F_r. If $\phi^r(t,j) \in D_r$, a jump according to G_r is triggered. In particular, the trajectory for $\phi^r_{\hat{z}}$ after jumps is given by

$$\phi^r_{\hat{z}}(t_j, j) = \phi^r_{\hat{z}}(t_j, j\text{-}1) + LM\big(\phi^r_z(t_j, j\text{-}1) - \phi^r_{\hat{z}}(t_j, j\text{-}1)\big) \tag{4.6}$$

at each $(t_j, j-1)$, $(t_j, j) \in \text{dom } \phi^r$.

For the solution ϕ with $\phi(0,0) \in \mathcal{W}_1 \cup \mathcal{W}_2$, if $\phi(t,j) \in C_a$ it flows according to F_a. If $\phi \in D_{a_1}$, a reset according to G_1 is triggered. The trajectory for $\phi_{\hat{z}}$ after jumps according to G_1 is given by,

$$\phi_{\hat{z}}(t_j, j) = \phi_{\hat{z}}(t_j, j-1) \tag{4.7}$$

at each $(t_j, j-1)$, $(t_j, j) \in \operatorname{dom} \phi$ for all $j \in \{2k : k \in \mathbb{N}_{>0}\}$ when $\phi(0,0) \in \mathcal{W}_1$ and for all $j \in \{2k+1 : k \in \mathbb{N}_{>0}\}$ when $\phi(0,0) \in \mathcal{W}_2$. If or when $\phi \in D_{a_2}$, $\phi(t_j, j)$ maps according to G_2 with $\phi_{\hat{z}}$ after jumps given by

$$\begin{aligned}\phi_{\hat{z}}(t_j, j) = \phi_{\hat{z}}(t_j, j\text{-}1) \\ + e^{A(\tau_O(t_j, j-1) - \phi_{\ell_{\tau_P}}(t_j, j-1))} L\Big(\phi_{\ell_y}(t_j, j\text{-}1) \\ - M e^{-A(\tau_O(t_j, j-1) - \phi_{\ell_{\tau_P}}(t_j, j-1))} \phi_{\hat{z}}(t_j, j\text{-}1)\Big)\end{aligned} \tag{4.8}$$

at each $(t_j, j-1)$, $(t_j, j) \in \operatorname{dom} \phi$ for all $j \in \{2k+1 : k \in \mathbb{N}_{>0}\}$ when $\phi(0,0) \in \mathcal{W}_1$ and for all $j \in \{2k : k \in \mathbb{N}_{>0}\}$ when $\phi(0,0) \in \mathcal{W}_2$.

Now, since $T^d = 0$ and $\phi_{\ell_{\tau_P}}(0,0) = \tau_O(0,0)$, the delay term $\tau_O(t,j) - \phi_{\ell_{\tau_P}}(t,j)$ in the expression for the update law in (4.8) is zero at each jump according to G_2 or for all $(t_j, j) \in \{(t,j) \in \operatorname{dom} \phi : t = t_j, j \in \mathcal{I}_m\}$. Furthermore, $\phi_{\ell_y}(0,0) = M\phi_z(0,0)$, thus $\phi_{\ell_y}(t_j, j) = M\phi_z(t,j)$ at each reset according to G_2 or for all $(t_j, j) \in \{(t,j) \in \operatorname{dom} \phi : t = t_j, j \in \mathcal{I}_m\}$. Then, (4.8) can be expressed as

$$\phi_{\hat{z}}\big(t_j, j\big) = \phi_{\hat{z}}(t_j, j\text{-}1) + LM\big(\phi_z(t_j, j\text{-}1) - \phi_{\hat{z}}(t_j, j\text{-}1)\big)$$

Noting the equivalence to the expression in (4.6), we can express $\phi_{\hat{z}}$ along jumps as a function of $\phi^r_{\hat{z}}$ as follows:

$$\phi_{\hat{z}}(t_j, j) = \begin{cases} \phi^r_{\hat{z}}(t_j, r_\phi(j\text{-}1)) & \forall j \in \mathcal{I}_d \\ \phi^r_{\hat{z}}(t_j, r_\phi(j)) & \forall j \in \mathcal{I}_m \end{cases}$$

Now, given identical flow dynamics in z, $\hat{z}$, and τ_N, one then has

$$\phi(t,j) = \big(\phi^r(t, r_\phi(j)), \phi_{\tau_\delta}(t,j), \phi_q(t,j), \phi_{\ell_y}(t,j), \phi_{\ell_{\tau_P}}(t,j)\big)$$

thus since solutions to $\mathcal{H}_r$ converge exponentially to $\mathcal{A}_r$ by [4, Theorem 1], it follows that

$$\lim_{t+j\to\infty} |\phi^r(t,j)|_{\mathcal{A}_r} = 0$$

moreover, given that $\mathcal{A}_r \subset \mathcal{A}_a$ it can be concluded that

$$\lim_{t+j\to\infty} |\phi(t,j)|_{\mathcal{A}_a} = 0$$

• **Proof of Non-conventional Case**

For solutions with initial conditions $\phi(0,0) \in (C_a \cup D_a) \setminus (\mathcal{W}_1 \cup \mathcal{W}_2)$, namely those with $\phi_{\ell_y}(0,0) \neq M\phi_z(0,0)$ and $\phi_{\ell_{\tau_P}}(0,0) \neq \tau_P(0,0)$, after a period of time $T^* \geq t+j$ the solution converges towards $\mathcal{A}_a$. Consider a solution ϕ with initial condition $\phi(0,0) \in \{x \in C_{a_2} \cup D_{a_2} : \ell_y \neq Mz, \ell_{\tau_P} \neq \tau_P(0,0)\}$. Since $T^d = 0$, $\phi(0,0) \in D_{a_2}$ and the solution jumps according to G_2. In particular, at $(t_1, 1)$,

$$\begin{aligned}\phi_{\hat{z}}(t_1,1) = \phi_{\hat{z}}(0,0) + e^{A(\tau_O(0,0)-\phi_{\ell_{\tau_P}}(0,0))} L\big(\phi_{\ell_y}(0,0) \\ - Me^{-A(\tau_O(0,0)-\phi_{\ell_{\tau_P}}(0,0))}\phi_{\hat{z}}(0,0)\big)\end{aligned}$$

with $\phi_{\ell_y}(0,0) \neq M\phi_z(0,0)$ and $\phi_{\ell_{\tau_P}}(0,0) \neq \tau_P(0,0)$, $\phi(t_1,1)$ may diverge away from $\mathcal{A}_a$. The solution then flows in the interval $[t_1,t_2] \times \{1\}$ until $\phi(t_2,1) \in D_{a_1}$, when the solution jumps according to G_1. In particular, at $(t_2,2)$, $\phi_{\ell_y}(t_2,2) = M\phi_z(t_2,1)$ and $\phi_{\ell_{\tau_P}}(t_2,2) = \tau_P(t_2,1)$ which means $\phi(t_2,2) \in \mathcal{W}_1 \cup \mathcal{W}_2$. Thus, we can show that for some $(t,j) \in \operatorname{dom}\phi$ such that $t+j \geq T^*$, $\phi(t,j) \in \mathcal{W}_1 \cup \mathcal{W}_2$. Moreover, following the proof for the conventional case, the solution converges to $\mathcal{A}_a$. □

4.2 Attractivity for delay solutions with synchronized clocks

With attractivity established for the nominal case, we now present attractivity to $\mathcal{A}_a$ for the delay case. Consider the Lyapunov function candidate from [4] defined for every $x_a \in \mathcal{X}_a$ as

$$V(x_a) = \varepsilon^{\mathsf{T}} e^{A^{\mathsf{T}}\tau_N} P e^{A\tau_N}\varepsilon \tag{4.9}$$

where $\varepsilon = z - \hat{z}$ and $P = P^{\mathsf{T}} \succ 0$. Then, given $\phi^\delta(0,0) \in C_a \cup D_a$, it can be shown that delay solutions $\phi^\delta \in \mathcal{S}^\delta_{\mathcal{H}_a}$ converge to the set $\mathcal{A}_a$, exponentially. Moreover, it can be shown that the Lyapunov function evaluated along a delay solution ϕ^δ for a given initial condition is bounded by the Lyapunov function evaluated along its nominal counterpart ϕ^{nom} (see Proposition A.0.3) and a bounded perturbation. To facilitate the analysis in the result that follows, let $\phi^{\text{nom}}_\varepsilon = \phi^{\text{nom}}_z - \phi^{\text{nom}}_{\hat{z}}$ and $\phi^\delta_\varepsilon = \phi^\delta_z - \phi^\delta_{\hat{z}}$ denote the trajectories of the state error for the respective nominal (ϕ^{nom}) and delay (ϕ^δ) solutions.

To assist with the analysis between the two solution types, given a solution to $\mathcal{H}_a$, we define a reparameterization function s_ϕ, given as follows:

If $\phi(0,0) \in C_{a_1} \cup D_{a_1}$

$$s_\phi(j) := \begin{cases} j & \forall j \in \mathcal{I}_d \\ j+1 & \forall j \in \mathcal{I}_m \end{cases}$$

If $\phi(0,0) \in C_{a_2} \cup D_{a_2}$

$$s_\phi(j) := \begin{cases} j & \forall j \in \mathcal{I}_m \\ j+1 & \forall j \in \mathcal{I}_d \end{cases}$$

The function s_ϕ allows to compare solutions ϕ^{nom} to $\mathcal{H}_a$ and ϕ^δ to $\mathcal{H}_a$.

Theorem 4.2.1. *Given the hybrid system $\mathcal{H}_a$ in (3.2) with $D_b = \emptyset$ and input pair $\tau_P \equiv \tau_O$ such that $\{t : (t,j) \in \text{dom}\,(\tau_P, \tau_O\}$ is unbounded, suppose that there exist $P = P^\top \succ 0$ such that T_2^N, T_1^N, L, and M satisfy condition (4.3). Then, for each $T^d \in [0, T_1^N]$, each solution ϕ to $\mathcal{H}_a$ with $D_b = \emptyset$ and input pair $\tau_P \equiv \tau_O$ is such that*

$$\lim_{t+j\to\infty} |\phi(t,j)|_{\mathcal{A}_a} = 0$$

Furthermore, there exist positive constants α and β such that each $\phi^\delta \in \mathcal{S}^\delta_{\mathcal{H}_a}$ with $D_b = \emptyset$ and input pair $\tau_P \equiv \tau_O$ satisfies

$$\begin{aligned} \alpha|\phi^\delta(t,j)|_{\mathcal{A}_a} \leq V\big(\phi^\delta(t,j)\big) \leq V\big(\phi^{\text{nom}}(t, s_\phi(j))\big) \\ + \beta \phi_\varepsilon^{\text{nom}}(t,j)^\mathsf{T} \phi_\varepsilon^{\text{nom}}(t,j) \end{aligned} \tag{4.10}$$

for each $(t,j) \in \text{dom}\,\phi^\delta$, where ϕ^{nom} is a nominal maximal solution for the same initial condition to ϕ^δ and $\phi_\varepsilon^{\text{nom}} = \phi_z^{\text{nom}} - \phi_{\hat{z}}^{\text{nom}}$.

Proof. Given matrices A, L, and M of appropriate dimensions and positive scalars $T^d \leq T_1^N \leq T_2^N$. Pick a solution ϕ^δ with initial condition $\phi^\delta(0,0) \in \{x_a \in C_a \cup D_a : \ell_y = Mz\}$ and its nominal counterpart ϕ^{nom} for the same initial condition and identical τ_N trajectories, i.e., $\phi^{\text{nom}}_{\tau_N}(t,j) = \phi^\delta_{\tau_N}(t,j)$ for all (t,j) dom ϕ^δ. Consider the Lyapunov function candidate (4.9). Then, let

$$\begin{aligned} V^{\text{nom}}(t, s_\phi(j)) &:= V(\phi^{\text{nom}}(t, s_\phi(j))) \quad \forall (t,j) \in \text{ dom } \phi^\delta \\ V^\delta(t,j) &:= V(\phi^\delta(t,j)) \qquad\qquad\qquad\quad \forall (t,j) \in \text{ dom } \phi^\delta \end{aligned}$$

Noting the relationship between ϕ^{nom} and ϕ^{δ} as established in Proposition A.0.3, let $V^{\delta}(t,j)$ be expressed as a perturbation of $V^{\text{nom}}(t, s_{\phi}(j))$, i.e.

$$V^{\delta}(t,j) = V(\phi^{\text{nom}}(t, s_{\phi}(j))) + \rho(t,j) \quad \forall (t,j) \in \text{ dom } \phi^{\delta}$$

Since $\phi^{\text{nom}}(t,j) = \phi^{\delta}(t,j)$ for all $(t,j) \in \mathcal{T}_1$ when the initial condition is in $C_{a_1} \cup D_{a_1}$ (see Proposition A.0.3). The quantity $\rho(t,j)$ is given by,

$$\rho(t,j) = \begin{cases} V(\phi^{\delta}(t,j)) - V(\phi^{\text{nom}}(t, s_{\phi}(j))) & \forall (t,j) \in \mathcal{T}_2 \\ 0 & \forall (t,j) \in \mathcal{T}_1 \end{cases}$$

Observe that for each $x_a \in C_a$, $\langle \nabla V(x_a), F_a(x_a) \rangle = 0$, therefore ρ remains constant during flows and can be expressed by its value at jumps as follows:

$$\rho(t,j) = \begin{cases} V(\phi^{\delta}(t_j,j)) - V(\phi^{\text{nom}}(t_{s_{\phi}(j)}, s_{\phi}(j))) & \forall (t,j) \in \mathcal{T}_2 \\ 0 & \forall (t,j) \in \mathcal{T}_1 \end{cases}$$

Before expanding ρ, note that the reparameterization of ϕ^{nom} onto the domain of ϕ^{δ} via $s_{\phi}(j)$ following each $(t_{j+1}, j) \in \mathcal{T}_1$, gives the nominal solution mapped according to G_2. In particular, one has

$$\begin{aligned} \phi_{\varepsilon}^{\text{nom}}(t_{s_{\phi}(j)}, s_{\phi}(j)) &= \phi_{z}^{\text{nom}}(t_{s_{\phi}(j)}, s_{\phi}(j\text{-}1)) \\ &\quad - \Big(\phi_{\hat{z}}^{\text{nom}}(t_{s_{\phi}(j)}, s_{\phi}(j\text{-}1)) + LM \Big(\phi_{z}^{\text{nom}}(t_{s_{\phi}(j)}, s_{\phi}(j\text{-}1)) \\ &\qquad - \phi_{\hat{z}}^{\text{nom}}(t_{s_{\phi}(j)}, s_{\phi}(j\text{-}1)) \Big) \Big) \\ &\qquad = (I - LM) \phi_{\varepsilon}^{\text{nom}}(t_{s_{\phi}(j)}, s_{\phi}(j\text{-}1)) \end{aligned}$$

at each $(t_j, s_{\phi}(j-1)), (t_j, s_{\phi}(j)) \in \text{dom } \phi^{\delta}$. For the same jump index j, that is, following each $(t_{j+1}, j) \in \mathcal{T}_1$, the delay solution $\phi_{\varepsilon}^{\delta}$ is given by

$$\phi_{\varepsilon}^{\delta}(t_j, j) = \phi_{z}^{\delta}(t_j, j\text{-}1) - \phi_{\hat{z}}^{\delta}(t_j, j\text{-}1)$$

at each $(t_j, j-1), (t_j, j) \in \text{dom } \phi^{\delta}$ for all $j \in \mathcal{I}_m$. Then, substituting the expressions into ρ leads to

$$\begin{aligned} \rho(t,j) &= V\big(\phi^{\delta}(t_j,j)\big) - V\big(\phi^{\text{nom}}(t_j,j)\big) \\ &= \phi_{\varepsilon}^{\delta}(t_j, j\text{-}1)^{\mathsf{T}} Q(t_j, j\text{-}1) \phi_{\varepsilon}^{\delta}(t_j, j\text{-}1) - \phi_{\varepsilon}^{\text{nom}}(t_{s_{\phi}(j)}, s_{\phi}(j\text{-}1))^{\mathsf{T}} \\ &\quad \times (I - LM)^{\mathsf{T}} Q(t_j, s_{\phi}(j\text{-}1)) (I - LM) \phi_{\varepsilon}^{\text{nom}}(t_{s_{\phi}(j)}, s_{\phi}(j\text{-}1)) \end{aligned}$$

where $Q(t,j) := e^{A^\mathsf{T}\tau_N(t,j)}Pe^{A\tau_N(t,j)}$. Then, since $\phi^{\text{nom}}(t,j) = \phi^\delta(t,j)$ for all $(t,j) \in \mathcal{T}_1$, we make the appropriate substitutions to get

$$\begin{aligned}\rho(t,j) = \phi_\varepsilon^{\text{nom}}(t_{s_\phi(j)}, s_\phi(j\text{-}1))^\mathsf{T}\Big(&Q(t_j, j-1)\\ &\text{-}(I\text{-}LM)^\mathsf{T}Q(t_{s_\phi(j)}, s_\phi(j\text{-}1))(I\text{-}LM)\Big)\phi_\varepsilon^{\text{nom}}(t_{s_\phi(j)}, s_\phi(j\text{-}1))\end{aligned}$$

Thus allowing ρ to be bounded as follows

$$|\rho(t,j)| \leq \beta\phi_\varepsilon^{\text{nom}}(t_{s_\phi(j)}, s_\phi(j\text{-}1))^\mathsf{T}\phi_\varepsilon^{\text{nom}}(t_{s_\phi(j)}, s_\phi(j\text{-}1)) \tag{4.11}$$

where

$$\beta := \max_{\tau_N \in [0, T_2^N]} \lambda_{\max}\big(e^{A^\mathsf{T}\tau_N}Pe^{A\tau_N}\big)|I\text{-}(I\text{-}LM)^\mathsf{T}(I\text{-}LM)|$$

which exists due to continuity of the matrix exponential. Then, one has

$$V^\delta(t,j) = \begin{cases} V\big(\phi^{\text{nom}}(t, s_\phi(j))\big) + \rho(t,j) & \forall (t,j) \in \mathcal{T}_2 \\ V\big(\phi^{\text{nom}}(t, s_\phi(j))\big) & \forall (t,j) \in \mathcal{T}_1 \end{cases}$$

In particular, one has

$$\alpha|\phi^\delta(t,j)|_{\mathcal{A}_a} \leq V\big(\phi^\delta(t,j)\big) \leq V\big(\phi^{\text{nom}}(t, s_\phi(j))\big) + \rho(t,j) \tag{4.12}$$

where

$$\alpha := \min_{v \in [0, T_2]} \lambda_{min}\big(e^{A^\mathsf{T}\tau_N}Pe^{A\tau_N}\big)$$

Now, since $\rho(t,j)$ decays to zero in the limit due to (4.11) and $\phi^{\text{nom}}(t, s_\phi(j))$ converges to the set $\mathcal{A}_a^{\text{nom}}$ via Proposition 4.1.1, then by the relations in (4.12) solutions ϕ^δ also converge to the set $\mathcal{A}_a$.

For the case of ϕ^δ solutions with initial condition $\phi^\delta(0,0) \in C_{a_2} \cup D_{a_2}$, the result follows from similar steps with $V^\delta(t,j)$ and $\rho(t,j)$ given by

$$V^\delta(t,j) = \begin{cases} V\big(\phi^{\text{nom}}(t, s_\phi(j))\big) + \rho(t,j) & \forall (t,j) \in \mathcal{T}_1 \\ V\big(\phi(t, s_\phi(j))\big) & \forall (t,j) \in \mathcal{T}_2 \end{cases}$$

where

$$\rho(t,j) = \begin{cases} V(\phi^\delta(t,j)) - V(\phi^{\text{nom}}(t, s_\phi(j))) & \forall (t,j) \in \mathcal{T}_1 \\ 0 & \forall (t,j) \in \mathcal{T}_2 \end{cases}$$

□

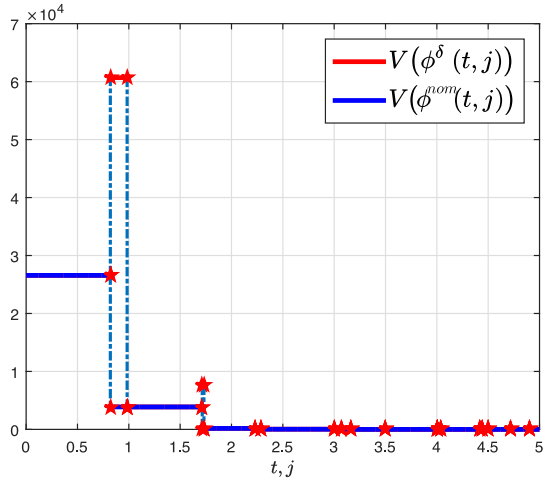

Figure 4.2: Plot of the Lyapunov trajectories of ϕ^r and ϕ.

Figure 4.2 illustrates the evolution of the function V along the trajectories for the two solution types. From the same initial condition, both solutions flow together. Then the solutions separate with the nominal solution (blue) decreasing upon measurement retrieval and the delayed solution (red) diverging due to the measurement delay. After some hybrid time, the delayed solution retrieves the delayed measurement and converges with the nominal solution. Example 5.0.2 illustrates Theorem 4.2.1 in Section 5.

4.3 Attractivity for delay solutions with clocks that synchronize in finite time.

In this section, we present our results for the case where the clock inputs τ_P and τ_O to $\mathcal{H}_a$ are not necessarily the same initially, but eventually synchronize in finite time (see Remark 4.3.4). The first result establishes attractivity to $\mathcal{A}_a$ for $\mathcal{H}_a$ with $D_b = \emptyset$ and input pair (τ_P, τ_O) satisfying conditions such that solutions to $\mathcal{H}_a$ are complete and the input pair synchronize in finite time. In the result that follows, we show attractivity to a set of interest for the full hybrid system $\mathcal{H}$ with conditions on the clock synchronization subsystem $\mathcal{H}_b$ such that the solutions to $\mathcal{H}$ are complete and the clock inputs to the subsystem $\mathcal{H}_a$ synchronize in finite time.

For the following results we will distinguish between solutions to $\mathcal{H}_a$ and solutions

to $\mathcal{H}$ by denoting

$$\phi_a \in \mathcal{S}_{\mathcal{H}_a}$$

and

$$\phi \in \mathcal{S}_{\mathcal{H}}$$

Proposition 4.3.1. *Given the hybrid system $\mathcal{H}_a$ in (3.2), suppose that there exist $P = P^\top \succ 0$ such that T_2^N, T_1^N, L, and M satisfy condition (4.3). Then, for each $T^d \in [0, T_1^N]$ and each input pair (τ_P, τ_O) to $\mathcal{H}_a$ satisfying*

B1) $\{t : (t, j) \in dom\ (\tau_P, \tau_O)\}$ is unbounded, and

B2) there exists $T^* \geq 0$ such that

$$\tau_P(t, j) = \tau_O(t, j)$$

for all $t + j \geq T^*$

each solution ϕ_a to $\mathcal{H}_a$ with input pair (τ_P, τ_O) and $D_b = \emptyset$ is such that

1. *$\{t : (t, j) \in dom\ \phi_a\}$ is unbounded, and*
2. *$\lim_{t+j\to\infty} |\phi_a(t, j)|_{\mathcal{A}_a} = 0$.*

Proof. To prove item 1), we will disprove the impossibility of a maximal solution to $\mathcal{H}_a$ with input pair (τ_P, τ_O) and $D_b = \emptyset$ to flow for arbitrarily large t. To this end, suppose there exists such a solution with input pair (τ_P, τ_O) satisfying B1). Then, $\{t : (t, j) \in \text{dom } \phi_a\}$ is bounded. The existence of such a solution implies that either

a) ϕ_a is not Zeno and died after finite time t, this further implies that either

a.1) G_a (with $D_b = \emptyset$ mapped the solution ϕ_a to a point outside of $C_a \cup D_a$; or

a.2) the solution ϕ_a died at a point in $C_a \setminus D_a$, at which F_a points outward of C_a;

or

b) ϕ_a is Zeno with $t \nearrow t_Z \notin \{t : (t, j) \in \text{dom } \phi_a\}$ as $j \to \infty$

Case a.1) does not happen due to (τ_P, τ_O) satisfying B1) and, by Lemma 3.0.4 item 1), G_a cannot map points in D_a outside of $C_a \cup D_a$ with $D_b = \emptyset$. Moreover, a.2) does not happen since (τ_P, τ_O) satisfies B1) and, by Lemma 3.0.4 item 2), $F_a(x_a) \subset T_{C_a}(x)$ for each x_a such that $x \in C_a \setminus D_a$. Case b) does not happen since (τ_P, τ_O) satisfies B1) and after any reset of ϕ_a via $\phi_a(t_j, j) = G_2(\phi_a(t_j, j\text{-}1), \tau_P)$ then for the same t_j there exists t_{j+1} such that $0 < T_1^N \leq t_{j+1} - t_j \leq T_2^N - T^d$ (see Remark A.0.1). Therefore, it must be the case that the solution ϕ_a to $\mathcal{H}_a$ with input pair (τ_P, τ_O) satisfying B1) is such that $\{t : (t, j) \in \text{dom } \phi_a\}$ is unbounded. This contradicts our assumption that $\{t : (t, j) \in \text{dom } \phi_a\}$ is bounded and concludes the proof of item 1).

To prove item 2), pick a maximal solution $\phi_a \in \mathcal{S}_{\mathcal{H}_a}$ with input pair (τ_P, τ_O) satisfying B1) and B2) with $D_b = \emptyset$. By item 1), $\{t : (t, j) \in \text{dom } \phi_a\}$ is unbounded. Moreover, by Lemma 3.0.4, $\phi_a(t, j) \in C_a \cup D_a$ for all $(t, j) \in \text{dom } \phi_a$. Now observe, for $t + j \geq T^*$, the conditions in Theorem 4.2.1 are satisfied since condition (4.3) is satisfied and the inputs (τ_P, τ_O) satisfy B2). Therefore, by Theorem 4.2.1, item 2) holds. □

Theorem 4.3.2. *Given the hybrid system $\mathcal{H}$ in 3.1, suppose that there exist $P = P^\top \succ 0$ such that T_2^N, T_1^N, L, and M satisfy condition (4.3). Suppose further that the subsystem $\mathcal{H}_b$ in (3.3) is such that*

1. *every maximal solution ϕ to $\mathcal{H}$ is complete, and*
2. *condition B2) in Proposition 4.3.1 holds;*

Then, for each $T^d \in [0, T_1^N]$, each maximal solution ϕ to $\mathcal{H}$ is such that

$$\lim_{t+j \to \infty} |\phi(t, j)|_{\mathcal{A}} = 0$$

where $\mathcal{A} := \mathcal{A}_a \times \mathbb{R}_{\geq 0} \times \mathbb{R}_{\geq 0} \times \mathcal{M}$.

Proof. Pick a maximal solution ϕ to $\mathcal{H}$. By Lemma 3.0.4, $\phi_{x_a}(t, j) \in C_a \cup D_a$ for all $(t, j) \in \text{dom } \phi$ since ϕ does not escape in finite time. For $t + j \geq T^*$, the conditions in Proposition 4.3.1 for the hybrid subsystem $\mathcal{H}_a$ are satisfied since (4.3) is satisfied and $\mathcal{H}_b$ renders $\phi_{\tau_P}(t, j) = \phi_{\tau_O}(t, j)$ for all $t + j \geq T^*$. Then by Proposition 4.3.1, $\lim_{t+j \to \infty} |\phi(t, j)|_{\mathcal{A}} = 0$. □

Remark 4.3.3. *Observe that this result builds on the design of the nominal system $\mathcal{H}_a$ for synchronized clock inputs by interconnecting it with $\mathcal{H}_b$ representing a finite time clock synchronization algorithm (see Remark 4.3.4) that satisfies the conditions in Theorem 4.3.2. As noted in Section 1.2, the authors of [19] provide LMI conditions that renders a similar observer-based networked system with variable delays, stable for a bounded clock synchronization error. However, as the authors note in their results, the design of the observer and controller gains to satisfy the associated LMI conditions are not straightforward. We remind the reader that our approach uses a tractable LMI condition (4.3) (see algorithm in [4]) and a finite time clock synchronization algorithm for which several solutions exist.*

Remark 4.3.4. *Concerning the existence of finite time clock synchronizations implementable in $\mathcal{H}$, we point the reader to the IEEE 1588 precision time protocol design for networked control system in [22] and firefly-based algorithms as given in [23] both of which guarantee synchronization in finite time.*

Chapter 5

Examples

Example 5.0.1. *Recall the system data from the motivation example in Section 1.1,* $A = 1$, $M = 1$, $L = 1 - e^{-1}$ *with constants* $T_1^N = T_2^N = 1$. *Then, let* $T^d = 0.2$. *Simulating the system* $\mathcal{H}_a$ *with synchronized clock inputs* τ_P *and* τ_O, *the estimate converges even in the presence of measurements delays as shown in Figure 5.1. Recall that this was not the case in the example presented in the introduction.* [1]

Example 5.0.2. *Consider an oscillatory autonomous system given by* $A = \begin{bmatrix} 0 & 1 \\ -1 & 0 \end{bmatrix}$ *and matrix* $M = \begin{bmatrix} 1 & 0 \end{bmatrix}$ *with timer bounds* $T^d = T_1^N = 0.2$, $T_2^N = 1$. *Using the design algorithm outlined in [4] for the given parameters, the gain matrix is given by* $L = \begin{bmatrix} 1.0097 & 0.6015 \end{bmatrix}^\mathsf{T}$.

Starting with the case of synchronized clocks, i.e. $\phi(0,0) \in C_1 \cup D_1$ *such that* $\phi_{\tau_P}(0,0) = \phi_{\tau_O}(0,0)$, *Figure 5.2 depicts the error in each state component for* ϕ^{nom} *and* ϕ^δ *and shows the norm of the error for the two solutions, in addition the bound in (4.10) is plotted to demonstrate the asymptotic attractivity of* ϕ^δ.

As discussed in Section A, the two trajectories flow together from the initial condition, at the first jump the error on the estimate for ϕ^{nom} *decreases due to the measurement arrival at broadcast while* ϕ^δ *continues flowing. At the next jump the error for* ϕ^δ *decreases due to the arrival of the delay measurement and then resumes flowing with* ϕ^{nom}.

For the case where the clock nodes are not synchronized i.e. $\phi(0,0) \in C_1 \cup D_1$ *such that* $\phi_{\tau_P}(0,0) \neq \phi_{\tau_O}(0,0)$, *consider a simulation of the full system* $\mathcal{H}$ *where* $\mathcal{H}_b$

[1] Code at github.com/HybridSystemsLab/HybridObsScalarPlant

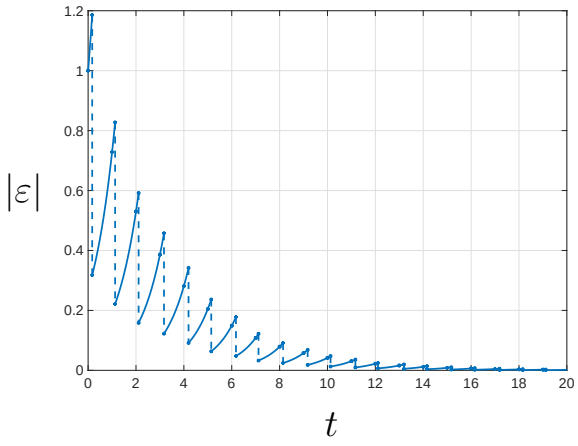

Figure 5.1: The evolution of the estimation error with respect to hybrid time. The vertical dashes represent the resets of $\hat{z}$ according to $\hat{z}^+$ in (1.5).

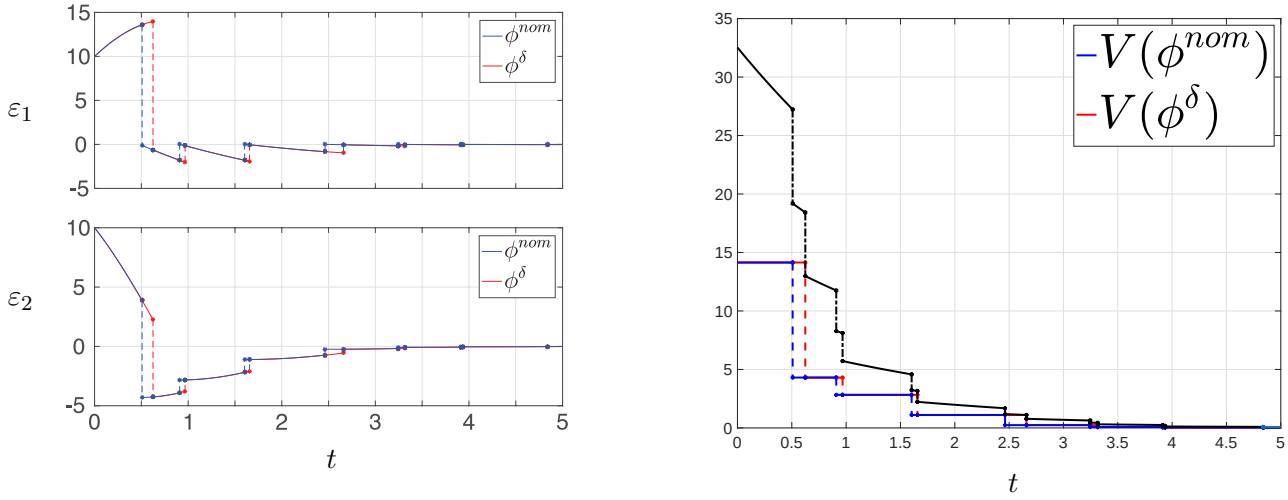

Figure 5.2: Plot of the error on the state components (left) and of $V(x)$ evaluated along the trajectories of ϕ^{nom} and ϕ^{δ} (right) for synchronized clocks from Example 5.0.2. Furthermore, a plot of the bound from (4.10) plotted in black.

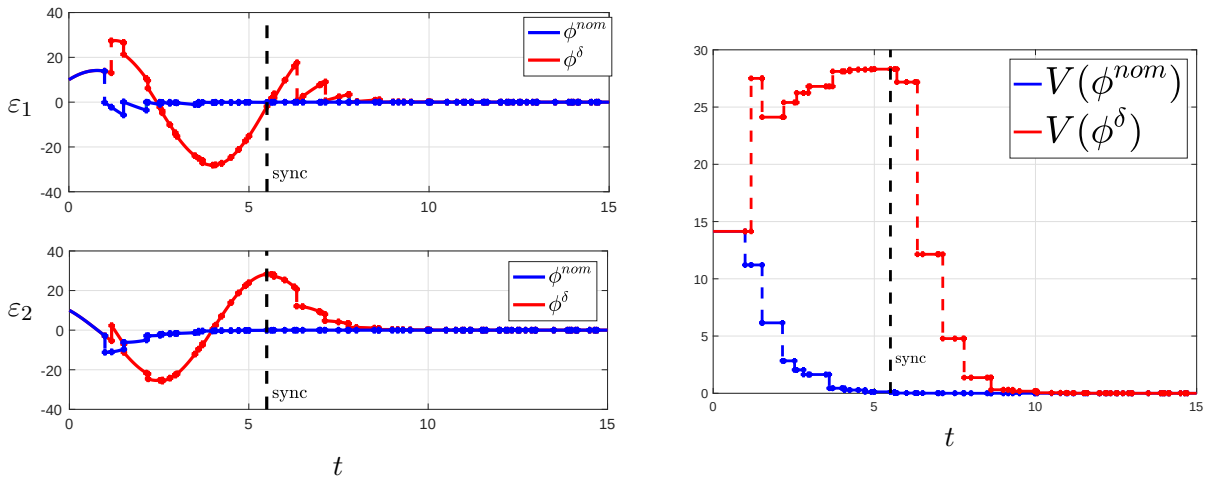

Figure 5.3: Plot of the error on the state components (left) and of $V(x)$ evaluated along the trajectories of ϕ^{nom} and ϕ^{δ} (right) for the case of initially mismatched clocks τ_P and τ_O.

is a model representation of the IEEE 1588 protocol, see [24] for details on the model. Figure 5.3 presents the error norm trajectories and displays the error in the components for both ϕ^{nom} *and* ϕ^{δ}.

In both figures, the trajectories flow together from the initial condition, at the first jump the estimation error for ϕ^{nom} *decreases while* ϕ^{δ} *continues flowing. In the sequence of jumps that follow, the error on the estimate of* ϕ^{nom} *converges to zero. The error on the estimate of* ϕ^{δ} *however, increases until the clocks are synchronized as marked by the dashed line denoted 'sync'. In the jumps that follow from the synchronization point, the error estimate of* ϕ^{δ} *converges toward zero.*

Example 5.0.3. *To demonstrate the flexibility of the system to account for a scenario of drifting clocks, consider the same system from the previous example but with a drifting observer clock i.e.* $\dot{\tau}_O = 1+\gamma$ *where* $\gamma = 0.001$. *In Figure 5.4, the error norm of the two trajectories for the simulation is given. Note the periodic synchronization of the plant and observer clocks prevents the drift in the observer clock from adversely affecting the norm of the error on the estimate for the delay solution.*[2]

[2]Code at github.com/HybridSystemsLab/HybridObsPlanarPlant

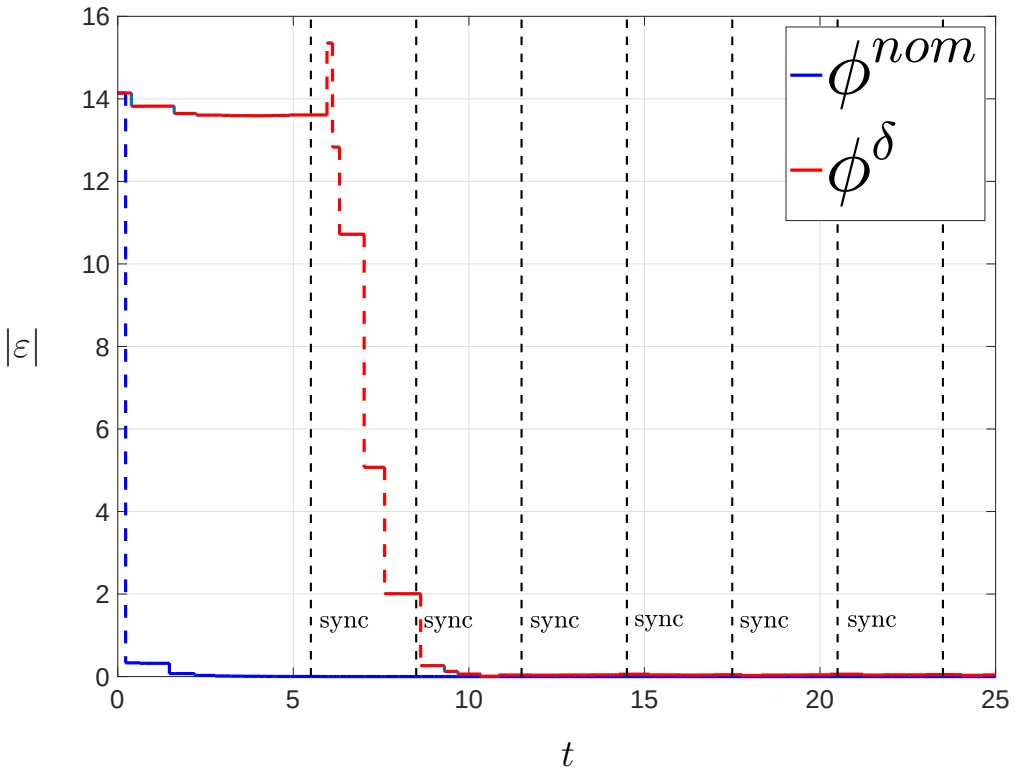

Figure 5.4: Plot of he error norm for ϕ^{nom} and ϕ^{δ} with drifting τ_O clock.

Chapter 6

Conclusion

In this thesis, we modeled an NCS with aperiodic sampling and network delays in a state estimation setting, using the hybrid systems framework in [20]. We proposed a modified state estimation algorithm for such a setting and a method to include a clock synchronization scheme. Results were given to show the model's equivalence to an NCS with aperiodic sampling and no network delay. Results were also provided regarding its asymptotic attractivity to a set of interest in the presence of network delays and initially mismatched clocks that eventually synchronize. Numerical results validating the theoretical findings were also given. Future works include a thorough analysis of the effect of measurement noise.

Bibliography

[1] J. P. Hespanha, P. Naghshtabrizi, and Y. Xu, "A survey of recent results in networked control systems," vol. 95, pp. 138–162, Jan 2007.

[2] W. Zhang, M. S. Branicky, and S. M. Phillips, "Stability of networked control systems," vol. 21, pp. 84–99, Feb 2001.

[3] P. Seiler and R. Sengupta, "Analysis of communication losses in vehicle control problems," in *Proceedings of the 2001 American Control Conference. (Cat. No.01CH37148)*, vol. 2, pp. 1491–1496 vol.2, 2001.

[4] F. Ferrante, F. Gouaisbaut, R. G. Sanfelice, and S. Tarbouriech, "State estimation of linear systems in the presence of sporadic measurements," *Automatica*, vol. 73, pp. 101 – 109, 2016.

[5] L. A. Montestruque and P. J. Antsaklis, "On the model-based control of networked systems," vol. 39, pp. 1837 – 1843, 2003.

[6] L. Hetel, J. Daafouz, J. Richard, and M. Jungers, "Delay-dependent sampled-data control based on delay estimates," *Systems and Control Letters*, vol. 60, no. 2, pp. 146 – 150, 2011.

[7] K. Y. Guisheng Zhai, Bo Hu and A. N. Michel, "Qualitative analysis of discrete-time switched systems," in *Proceedings of the 2002 American Control Conference (IEEE Cat. No.CH37301)*, vol. 3, pp. 1880–1885 vol.3, May 2002.

[8] R. M. Jungers, A. Kundu, and W. Heemels, "Observability and controllability analysis of linear systems subject to data losses," IEEE, 2017.

[9] A. S. Matveev and A. V. Savkin, "The problem of state estimation via asynchronous communication channels with irregular transmission times," *IEEE Transactions on Automatic Control*, vol. 48, pp. 670–676, April 2003.

[10] T. C. Mei Yu, Long Wang and F. Hao, "An lmi approach to networked control systems with data packet dropout and transmission delays," in *2004 43rd IEEE Conference on Decision and Control (CDC) (IEEE Cat. No.04CH37601)*, vol. 4, pp. 3545–3550 Vol.4, Dec 2004.

[11] A. R. Teel, "Connections between razumikhin-type theorems and the iss nonlinear small gain theorem," *IEEE Transactions on Automatic Control*, vol. 43, pp. 960–964, July 1998.

[12] Q.-L. H. Dong Yue and C. Peng, "State feedback controller design of networked control systems," *IEEE Transactions on Circuits and Systems II: Express Briefs*, vol. 51, pp. 640–644, Nov 2004.

[13] D. Nesic and A. R. Teel, "Input-output stability properties of networked control systems," vol. 49, pp. 1650–1667, Oct 2004.

[14] D. Nesic, A. R. Teel, and D. Carnevale, "Explicit computation of the sampling period in emulation of controllers for nonlinear sampled-data systems," *IEEE Transactions on Automatic Control*, vol. 54, pp. 619–624, March 2009.

[15] T. Ahmed-Ali, R. Postoyan, and F. Lamnabhi-Lagarrigue, "Continuousdiscrete adaptive observers for state affine systems," *Automatica*, vol. 45, no. 12, pp. 2986 – 2990, 2009.

[16] Y. Li and R. G. Sanfelice, "A robust finite-time convergent hybrid observer for linear systems," in *52nd IEEE Conference on Decision and Control*, pp. 3349–3354, Dec 2013.

[17] D. Dai and D. Nei, "Observer design for wired linear networked control systems using matrix inequalities," *Automatica*, vol. 44, no. 11, pp. 2840 – 2848, 2008.

[18] W. Zhang and M. S. Branicky, "Stability of networked control systems with time-varying transmission period.," in *In 39th Annual Allerton Conference on Communication Control and Computing*, vol. 39, p. 12051214 Vol.39, 2001.

[19] A. Seuret and K. H. Johansson, "Networked control under time-synchronization errors," in *Time Delay Systems: Methods, Applications and New Trends*, pp. 369–381, Springer, 2012.

[20] R. Goebel, R. G. Sanfelice, and A. R. Teel, *Hybrid Dynamical Systems: Modeling, Stability, and Robustness*. Princeton University Press, 2012.

[21] J. Chai and R. G. Sanfelice, "Forward invariance of sets for hybrid dynamical systems (Part I)," *To appear in IEEE Transactions on Automatic Control*, 2019.

[22] IEEE, "IEEE standard for a precision clock synchronization protocol for networked measurement and control systems," *IEEE Std 1588-2008 (Revision of IEEE Std 1588-2002)*, pp. 1–300, July 2008.

[23] Y. Li and R. G. Sanfelice, "Finite time stability of sets for hybrid dynamical systems," *Automatica*, vol. 100, pp. 200–211, 02/2019 2019.

[24] M. Guarro, F. Ferrante, and R. G. Sanfelice, "A hybrid observer for linear systems under delayed sproadic measurements," *Technical Report*, 2019.

[25] L. Hetel, C. Fiter, H. Omran, A. Seuret, E. Fridman, J.-P. Richard, and S. I. Niculescu, "Recent developments on the stability of systems with aperiodic sampling: An overview," *Automatica*, vol. 76, pp. 309 – 335, 2017.

[26] D. Luenberger, "An introduction to observers," vol. 16, pp. 596–602, Dec 1971.

[27] P. Naghshtabrizi and J. P. Hespanha, *Implementation Considerations For Wireless Networked Control Systems*, pp. 1–27. New York, NY: Springer New York, 2011.

[28] M. Cloosterman, N. van de Wouw, M. Heemels, and H. Nijmeijer, "Robust stability of networked control systems with time-varying network-induced delays," in *Proceedings of the 45th IEEE Conference on Decision and Control*, pp. 4980–4985, Dec 2006.

[29] D. Bernstein, *Matrix Mathematics: Theory, Facts, and Formulas - Second Edition.* Princeton University Press, 2009.

[30] W. P. M. H. Heemels, A. R. Teel, N. van de Wouw, and D. Nesic, "Networked control systems with communication constraints: Tradeoffs between transmission intervals, delays and performance," *IEEE Transactions on Automatic Control*, vol. 55, pp. 1781–1796, Aug 2010.

Appendix A

Properties of $\mathcal{H}_a$ for Synchronized Clocks

In this section, we present properties of the observer subsystem $\mathcal{H}_a$ to facilitate the analysis of the proposed observer algorithm in the main results. The ability of the proposed observer to converge to the state z depends on the clocks τ_P and τ_O eventually synchronizing. Thus, for the properties that follow, we consider $\mathcal{H}_a$ with given τ_P and τ_O input trajectories, such that the two clocks are synchronized, i.e., $\tau_P \equiv \tau_O$. See Remark 4.3.4.

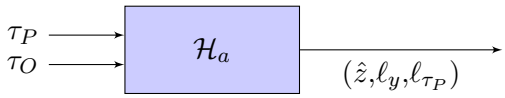

Figure A.1: Diagram of $\mathcal{H}_a$ in isolation.

Remark A.0.1. *Each solution $\phi^\delta \in \mathcal{S}^\delta_{\mathcal{H}_a}$ has flow intervals whose length is determined by the values of τ_N and τ_δ after they jump. Its domain is given as*

$$\text{dom } \phi^\delta = \bigcup_{j\in\mathbb{N}} \left([t^\delta_j, t^\delta_{j+1}] \times \{j\}\right)$$

where $t^\delta_0 = 0 \leq t^\delta_1 \leq \ldots \leq t^\delta_j$ is the sequence of strictly increasing and unbounded time instants for delay maximal solutions ϕ^δ. Due to the jumps being triggered by two different timers we note two types of bounds on the intervals of the time domain. Specifically,

when $\phi^\delta(0,0)$ is in $C_{a_1} \cup D_{a_1}$, one has

$$\begin{aligned} 0 &\leq t_1^\delta \leq T_2^N \\ 0 &\leq t_{j+1}^\delta - t_j^\delta \leq T^d \qquad\quad \forall j \in \mathcal{I}_m \\ T_1^N &\leq t_{j+1}^\delta - t_j^\delta \leq T_2^N - T^d \quad \forall j \in \mathcal{I}_d \end{aligned}$$

For the time domain of solutions from $\phi^\delta(0,0) \in C_{a_2} \cup D_{a_2}$, the following bounds hold:

$$\begin{aligned} 0 &\leq t_1^\delta \leq T^d \\ T_1^N &\leq t_{j+1}^\delta - t_j^\delta \leq T_2^N - T^d \quad \forall j \in \mathcal{I}_m \\ 0 &\leq t_{j+1}^\delta - t_j^\delta \leq T^d \qquad\quad \forall j \in \mathcal{I}_d \end{aligned}$$

Remark A.0.2. *For solutions $\phi^{\text{nom}} \in \mathcal{S}^{\text{nom}}_{\mathcal{H}_a}$, flow intervals depend solely on the value of τ_N after jumps. In particular*

$$\text{dom } \phi^{\text{nom}} = \bigcup_{j \in \{2k : k \in \mathbb{N}\}} \left([t_j^{\text{nom}}, t_{j+1}^{\text{nom}}] \times \{j\}\right) \cup \{(t_{j+1}^{\text{nom}}, j+1)\}$$

where

$$\begin{aligned} T_1^N &\leq t_{j+1}^{\text{nom}} - t_j^{\text{nom}} \leq T_2^N \quad \forall j \in \{k \geq 1 : k \in \mathbb{N}\} \\ 0 &\leq t_1^{\text{nom}} \leq T_2^N \end{aligned}$$

Given the two solution types, for a chosen delay maximal solution ϕ^δ, there exists a nominal maximal solution ϕ^{nom} for which the two solutions coincide over particular intervals of flow. More formally, we have the following result whose proof can be found in [24].

Proposition A.0.3. *For each delay solution $\phi^\delta \in \mathcal{S}^\delta_{\mathcal{H}_a}$, there exists a nominal solution $\phi^{\text{nom}} \in \mathcal{S}^{\text{nom}}_{\mathcal{H}_a}$ such that*

1) If $\phi(0,0) \in C_{a_1} \cup D_{a_1}$, then $\phi^{\text{nom}}(t,j) = \phi^\delta(t,j)$ for all $(t,j) \in \mathcal{T}_1$ where

$$\mathcal{T}_1 := \bigcup_{j \in \{2k : k \in \mathbb{N}\}} \left([t_j^\delta, t_{j+1}^\delta] \times \{j\}\right)$$

2) If $\phi(0,0) \in C_{a_2} \cup D_{a_2}$, then $\phi^{\text{nom}}(t,j) = \phi^\delta(t,j)$ for all $(t,j) \in \mathcal{T}_2$ where

$$\mathcal{T}_2 := \bigcup_{j \in \{2k+1 : k \in \mathbb{N}\}} \left([t_j^\delta, t_{j+1}^\delta] \times \{j\}\right)$$

where the sequence $t_0^\delta = 0 \leq t_1^\delta \leq \ldots \leq t_j^\delta$ *defines* dom ϕ^δ.

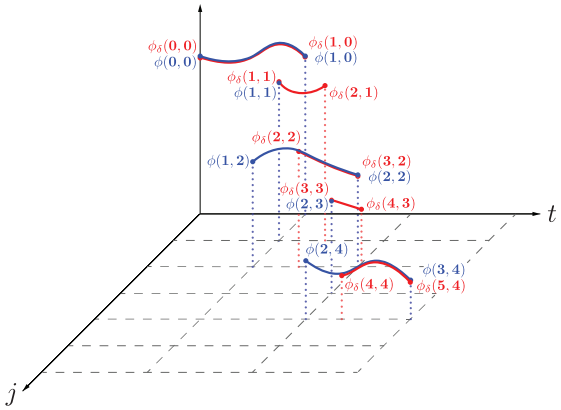

Figure A.2: Sample plot of the two solutions ϕ^{nom} and ϕ^δ showing the overlap over particular intervals of flow.